

**Study of Preferential Weld Corrosion in X52 Mild Steel with the  
Presence of Acetic Acid**

By

THINESHRAAJ JAYA RAMAN

16371

Dissertation submitted in partial fulfilment of the requirements for the  
Bachelor of Engineering (Hons)  
(Mechanical)

JANUARY 2016

Universiti Teknologi PETRONAS  
32610, Bandar Seri Iskandar,  
Perak

CERTIFICATION OF APPROVAL

**Study of Preferential Weld Corrosion in X52 Mild Steel with the Presence of  
Acetic Acid**

By

THINESHRAAJ NAIDU JAYA RAMAN

A project dissertation submitted to the  
Mechanical Engineering Programme  
Universiti Teknologi PETRONAS  
in partial fulfilment of the requirements for the  
BACHELOR OF ENGINEERING (Hons)  
(MECHANICAL ENGINEERING)

Approved by:

---

(DR. KEE KOK ENG)

UNIVERSITI TEKNOLOGI PETRONAS  
TRONOH, PERAK  
JANUARY 2016

## **CERTIFICATION OF ORIGINALITY**

This is to certify that I am responsible for the work submitted in this project, that the original work is my own except as specified in the references and acknowledgements, and that the original work contained herein have not been undertaken or done by unspecified sources or person.

---

THINESHRAAJ NAIDU JAYARAMAN

## ABSTRACT

Preferential weld corrosion occurs in the hydrocarbon carrying pipelines due to CO<sub>2</sub> presence. The weld segments consist of parent metal, HAZ and weld metal that causes corrosion due to potential difference. The corrosion could be mitigated with the formation of protective layer (FeCO<sub>3</sub>). However, the mitigation has not been effective as the FeCO<sub>3</sub> layer formation is disrupted by environmental conditions like the pH and also the presence of weak acids like Acetic Acid (HAc) The purpose of this research is to investigate the presence of HAc and its effect on the corrosion rate of the weld segments. The influence of pH on the FeCO<sub>3</sub> formation on the weld segments with and without HAc present is also analyzed. A coupled sample and an un-coupled sample is prepared from the API 5L X52 mild steel weld segment. Test parameters were set to varying pH 4 and 6.6 with and without 1000ppm HAc present. 4 glass cells are set up to measure the intrinsic corrosion rate of the un-coupled sample and 4 glass cells are set up to measure the galvanic corrosion rate of the coupled sample. Linear Polarization Resistance (LPR) was used to measure the intrinsic corrosion rate and the galvanic corrosion rate of the samples. The total corrosion rate of each weld region was obtained from the sum of intrinsic corrosion and galvanic corrosion. The surface morphology was studied using Scanning Electron Microscopy (SEM) and EDX method. It was found that without the presence of HAc, increasing the pH value from 4 to 6.6 causes 66% of total corrosion rate increment. With the presence of 1000ppm HAc, increasing the pH value from 4 to 6.6 causes total corrosion rate to increase by 62%. At constant pH 4, addition of 1000 ppm HAc increases the total corrosion rate by 55%. At constant pH 6.6, addition of 1000 ppm HAc increases the total corrosion rate by 50%. HAc presence at pH 6.6 forms thick spots of FeCO<sub>3</sub> on parent metal surface.

**Key Words:** *Heat Affected Zone (HAZ); Weld Metal (WM); Parent Metal (PM); Preferential Weld Corrosion (PWC); Galvanic Corrosion; Intrinsic Corrosion; Linear Polarization Resistance (LPR); Glass Cell*

## **ACKNOWLEDGEMENT**

I would like to express my gratitude to God for His kind blessings for my strength and determination in completing this Final Year Project (FYP). The project was successfully completed regardless of all the obstacles and hard-times throughout the past eight months. My supervisor, Dr. Kee Kok Eng has given me his expert guidance, continuous support and motivation in completing this project. He has been always there to correct my mistakes, share his knowledge and also guide me the proper way of thesis writing for the past eight months. Thank you Dr. Kee Kok Eng. Gratitude is also extended to FYP II coordinator, Dr. Tamiru Alemu Lemma and Head of Centre of Corrosion Research, Dr. Mokhtar Che Ismail for their effort in assisting me throughout.

Thirdly, I would like to voice out my gratitude to Universiti Teknologi PETRONAS (UTP) for providing me the facilities to conduct my study. I am thankful to Mechanical Engineering Department and Centre of Corrosion Research (CCR) of UTP for the support I have received when I was conducting this study. Not forgetting my fellow Research Associates Miss Prema, Mr. Fauzi Abdul Karim, Miss Noor A'in, Mr. Masri Asmi, Mr Jamalluhaq Puad, Miss Rafida Abdul Jaal and Miss Ijah from Centre of Corrosion Research (CCR) whom have guided me through thick and thin during the conduction of this study. Finally, much love and gratitude's to my family members and friends that never failed in helping me through time. The unflinching support from them caused me to complete this FYP. Not to forget those who are directly or indirectly involved in the completion of this project. Thank you very much.

## Table of Contents

<b>ABSTRACT</b>	<b>viii</b>
<b>ACKNOWLEDGEMENT</b>	<b>xi</b>
<b>CHAPTER 1 INTRODUCTION</b>	<b>7</b>
1.1 Background study	7
1.2 Problem Statement	9
1.3 Objective	10
1.4 Scope of Study	10
<b>CHAPTER 2 LITERATURE REVIEW</b>	<b>11</b>
2.1 Preferential Weld Corrosion	11
2.1.1 Parent metal	14
2.1.2 Heat Affected Zone	14
2.1.3 Weld Metal	14
2.2 Carbon Dioxide in Weld Corrosion	15
2.3 Acetic Acid in Carbon Dioxide Corrosion	18
2.4 pH value influence	19
2.5 Temperature influence on weld corrosion	20
2.6 Intrinsic Corrosion	21
2.7 Galvanic Corrosion	21
<b>CHAPTER 3 METHODOLOGY</b>	<b>22</b>
3.1 Project Work Flow	22
3.2 Sample Preparation	23
3.2.1 Galvanic Current (Coupled)	26
3.2.2 Intrinsic Current (Uncoupled)	26

3.3	Experiment Execution	27
3.4.1	Test Parameters	27
3.3.3	Experimental Setup	28
3.3.4	Experiment Procedures	29
3.3.5	Techniques of Evaluation	31
3.3.6	Linear Polarization Resistance (LPR)	32
3.3.7	Galvanic Corrosion Test	33
3.3.8	Intrinsic Corrosion	34
3.3.9	Total Corrosion rate	34
3.3.10	Project Activities and Key Milestones	35
3.3.11	Gantt Chart	37
<b>CHAPTER 4 RESULTS &amp; DISCUSSION</b>		41
4.1	Intrinsic Corrosion Rates	42
4.2	Galvanic Corrosion Rates	45
4.3	Total Corrosion Rate	49
4.4	Surface Morphology	53
<b>CHAPTER 5 CONCLUSION &amp; RECOMMENDATION</b>		57
5.1	Conclusion	57
5.2	Recommendation	58
<b>REFERENCES</b>		61
<b>APPENDICES</b>		62

## LIST OF FIGURES

Figure 1: An example of typical weld corrosion in the pipeline occurred due to CO <sub>2</sub> reaction	8
Figure 2: Schematic showing the regions of a heterogeneous weld	11
Figure 3 the microstructural difference between the weld segments under 100x magnification (a)parent metal (b) HAZ and (c)weld metal.	13
Figure 4: The Carbon dioxide corrosion mechanism.	17
Figure 5: Project work flow for the entire 28 weeks.	22
Figure 6: Grinded and polished weld segment has been etched using 3% Nital solution	23
Figure 7: The microstructural observation of weld segments using Optical Microscope (OM) with magnification 50x (a) parent metal (b) HAZ and (c) weld metal.	24
Figure 8: Demarcation line was constructed precisely in between the weld segments to have a better guideline when cutting.	24
Figure 9: Samples obtained from the weld segment sectioning. (a) Coupled sample.	25
Figure 10: Coupled weld sample.	26
Figure 11: Un-coupled weld sample.	26
Figure 12: General experimental set up equipped with working electrode, reference electrode, auxiliary electrode, thermometer, CO <sub>2</sub> bubbler, glass cell and hot plate for LPR and ZRA test.	30
Figure 13: Shows the connection between the electrodes and the Galvo Gill 12 for the ZRA test	33
Figure 14: The connection between electrodes and Galvo Gill 12 for the LPR test.	34
Figure 15: Test 1 intrinsic corrosion rate of uncoupled parent, HAZ, and weld metal with time at 80°C, 3 wt. % NaCl, 0 ppm HAc and pH 4.	42
Figure 16: Test 2 intrinsic corrosion rate of uncoupled parent, HAZ, and weld metal with time at 80°C, 3 wt. % NaCl, 0 ppm HAc and pH 6.6.	43
Figure 17: Test 3 intrinsic corrosion rate of uncoupled parent, HAZ, and weld metal with time at 80°C, 3 wt. % NaCl, 1000 ppm HAc and pH 4.	43



Figure 18: Test 4 intrinsic corrosion rate of uncoupled parent, HAZ, and weld metal with time at 80°C, 3 wt. % NaCl, 1000 ppm HAc and pH 6.6.	44
Figure 19: Test 1 galvanic corrosion rate of coupled parent, HAZ, and weld metal with time at 80°C, 3 wt. % NaCl, 0 ppm HAc and pH 4	46
Figure 20: Test 2 galvanic corrosion rate of coupled parent, HAZ, and weld metal with time at 80°C, 3 wt. % NaCl, 0 ppm HAc and pH 6.6	46
Figure 21: Test 3 galvanic corrosion rate of coupled parent, HAZ, and weld metal with time at 80°C, 3 wt. % NaCl, 1000 ppm HAc and pH 4.	47
Figure 22: Test 4 galvanic corrosion rate of uncoupled parent, HAZ, and weld metal with time at 80°C, 3 wt. % NaCl, 1000 ppm HAc and pH 6.6.	47
Figure 23: Intrinsic corrosion rate of parent, HAZ and weld.	45
Figure 24: Galvanic corrosion of parent, HAZ and weld.	48
Figure 25: Total corrosion rate of parent metal compared to the intrinsic corrosion rate and galvanic corrosion rate.	49
Figure 26: Total corrosion rate of HAZ metal compared to the intrinsic corrosion rate and galvanic corrosion rate.	50
Figure 27: Total corrosion rate of weld metal compared to the intrinsic corrosion rate and galvanic corrosion rate.	50
Figure 28: Test 1 coupled specimen surface morphology of (a) parent steel, (b) HAZ and (c) weld metal after 24 hours LPR test.	53
Figure 29: Test 2 coupled specimen surface morphology of (a) parent steel, (b) HAZ and (c) weld metal after 24 hours LPR test.	53
Figure 30: Test 3 coupled specimen surface morphology of (a) parent steel, (b) HAZ and (c) weld metal after 24 hours LPR test.	54
Figure 31: Test 4 coupled specimen surface morphology of (a) parent steel, (b) HAZ and (c) weld metal after 24 hours LPR test.	54
Figure 32: SEM micrograph showing the cross section of the FeCO <sub>3</sub> layer formed coupled sample under Test 2 experimental conditions. (a) parent metal surface;(b) HAZ surface;(c) weld metal surface;(d) EDX results.	55

- Figure 33: SEM micrograph showing the cross section of the  $\text{FeCO}_3$  layer formed coupled sample under Test 4 experimental conditions. (a) parent metal surface;(b) HAZ surface;(c) weld metal surface;(d) EDX results. 56
- Figure 34: Test 1 current weld measurement of coupled parent, HAZ, and weld metal with time at  $80^\circ\text{C}$ , 3 wt. % NaCl, 0 ppm HAc and pH 4. 62
- Figure 35: Test 2 current weld measurement of coupled parent, HAZ, and weld metal with time at  $80^\circ\text{C}$ , 3 wt. % NaCl, 0 ppm HAc and pH 6.6. 62
- Figure 36: Test 3 current weld measurement of coupled parent, HAZ, and weld metal with time at  $80^\circ\text{C}$ , 3 wt. % NaCl, 1000 ppm HAc and pH 4. 63
- Figure 37: Test 4 current weld measurement of uncoupled parent, HAZ, and weld metal with time at  $80^\circ\text{C}$ , 3 wt. % NaCl, 1000 ppm HAc and pH 6.6. 63

## LIST OF TABLES

Table 1: The compositional percentage (wt%) of parent metal and weld metal.	12
Table 2; The ratio and the surface area of the sectioned weld samples	25
Table 3: Test parameters designed for the conduction of the experiment.	27
Table 4: The milestones that has been achieved throughout the completion of the Final Year Project.	35
Table 5: Gantt chart of Final Year Project 1	38
Table 6: Gantt chart of Final Year Project 2	39
Table 7: shows the parameters of Test 1, Test 2, Test 3 and Test 4 that has been conducted in the basic conditions of 80°C, 3 wt.% NaCl, and 0.53 bar of CO <sub>2</sub> purging. The conditions of each test vary in terms of presence of HAc and pH value.	41
Table 8: Test parameters for 4 tests that has been conducted.	41
Table 9: The intrinsic corrosion rate of weld segments at initial point, final point and the average.	44
Table 10: The galvanic corrosion rate of weld segments at initial point, final point and the average.	48
Table 11: The intrinsic corrosion rate of weld segments at initial point, final point and the average.	64
Table 12: The galvanic corrosion rate of weld segments at initial point, final point and the average.	64

## CHAPTER 1

### INTRODUCTION

#### 1.1 Background study

Oil and gas industry needs underwater transportation pipelines for the flow of hydrocarbons across regions. In oil and gas, the pipelines are usually made from carbon steel and the joints are welded together. These pipelines undergo transport hydrocarbons under seawater environments. Damages due to internal pressure or any external forces could occur along the pipelines which may result in leakages and corrosion along the pipelines. During the maintenance processes, the pipelines with holes and cracks are welded as well. Welding at the elbows and along the hydrocarbon pipelines could have weld regions to be formed around the welded area.<sup>[1]</sup>

Preferential weld corrosion is a type of corrosion that could be induced from these welded regions. The galvanic differences between the welded regions form an electrochemical reaction to occur. The pipelines transport hydrocarbons that contain Carbon dioxide (CO<sub>2</sub>) and other form of weak acids, mainly Acetic Acid (HAc). Past research shows that the presence of these acidic gas and the HAc contributes to the corrosion induction in the pipelines. These presences cause the parent metal and the welded metal (HAZ and weld metal) to undergo an electrochemical reaction within them causing the corrosion to occur.<sup>[2]</sup>The Figure 1 below shows a weld corrosion that has occurred inside the pipeline.

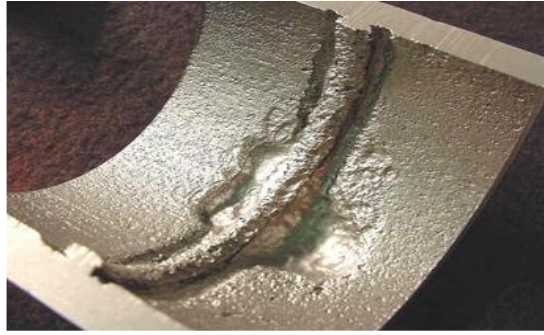


Figure 1: An example of typical weld corrosion in the pipeline occurred due to CO<sub>2</sub> reaction.

There are many precaution steps that has been taken by the worldwide oil and gas companies to mitigate the corrosion rates of their pipelines. Such methods would be as the usage of sacrificial anode and the usage of corrosion inhibitors. The precipitation of protective layer on the weld segment surface is one of the methods of mitigation to reduce the corrosion rate of pipelines. Formations of iron oxides ( $\text{Fe}_2\text{O}_3$ ), iron carbides ( $\text{Fe}_3\text{C}$ ) and iron carbonates ( $\text{FeCO}_3$ ) on the surface of the weld segment protects the weld segment from undergoing anodic reactions or corrosions. However, recent year studies show that the precipitation of this protective layers are disrupted with the presence of environmental conditions such as weak acids and pH regulation of the seawater. [Error! Reference source not found.]

The failure to mitigate the corrosion rate of the will cause catastrophic impact onto the pipelines. These corrosions start to grow and cause weakness in the pipeline mechanical properties such as the strength, ductility and impact strength. This could also cause the pipeline carbon steel to undergo loss of material, reduction in the thickness of the pipeline and sometimes ultimate failure. [2]

## 1.2 Problem Statement

As stated in the background study, preferential weld corrosion has many factors that affects the corrosion to occur. The most favorable mitigation process to control the preferential weld corrosion would be the natural way of mitigating, with is the formation of protective layer onto the surface of the weld segments.<sup>[Error! Reference source not found.]</sup> However, this process of mitigating weld corrosion has not been much effective as the cathode layer formation is being disrupted by environmental conditions like the pH value and also the presence of weak acids like Acetic Acid (HAc).

Many experiments have been conducted individually on finding the factors that cause preferential weld corrosion and factors that disrupts the formation of the protective layer. Based on the research done, it has been found that no study has been done on the effect of pH and Acetic Acid (HAc) with the cathodic layer formation on the surface of the weld segments. The questions that was risen based on studied papers would be;

1. Does presence of Acetic Acid (HAc) affect the formation of  $\text{FeCO}_3$  on to the surface of weld segments?
2. What is the effect of pH value on weld segment corrosion rate with the presence of Acetic Acid (HAc)?

### **1.3 Objective**

There are 2 objectives that needed to be achieved in this final year project;

1. To investigate the presence of Acetic Acid (HAc) and its effect on the corrosion rate of the weld segments.
2. To analyze the influence of pH on the  $\text{FeCO}_3$  formation on the weld segments.
3. To perform surface analysis of weld segment under the presence of HAc and pH influence.

### **1.4 Scope of Study**

Scope for this project has been identified as the following:

This topic of Final year project enables engineering student to cover one small critical area in the oil and gas industries. This investigation on the preferential weld corrosion with the presence of Acetic Acid could help the industry to discover the mitigation method towards corrosion by the formation of protective layer on the weld segments. The findings from this study is to be used in in the hydrocarbon pipeline industry to reduce the maintenance cost and also to improve the performance of equipment's in the oil and gas industry. The study could enhance the author's knowledge in the oil and gas pipeline industry and also prepare for the real life working environment.

## CHAPTER 2

### LITERATURE REVIEW

#### 2.1 Preferential Weld Corrosion

Welding plays a vital role in the oil and gas sector. The process is involved in the construction of pipelines, production tubing's and other pipeline operations. The welding process is to combine metal bodies by melting a filler material in between two structures at high temperature.<sup>[1]</sup> Carbon steels are by far the most commonly used material to build pipelines in the oil and gas industries. The common types of carbon steel are the X65 and the X52 type where it is cheaper and the mechanical properties of the carbon is suitable to be constructed into underwater oil and gas pipelines carrying hydrocarbons. However, carbon steel is frequently welded metals in the industry. These types of steels all forms of corrosion depending on the environment it is exposed to.<sup>[2]</sup> The Figure 2 below show schematic view of a heterogeneous weld segment.

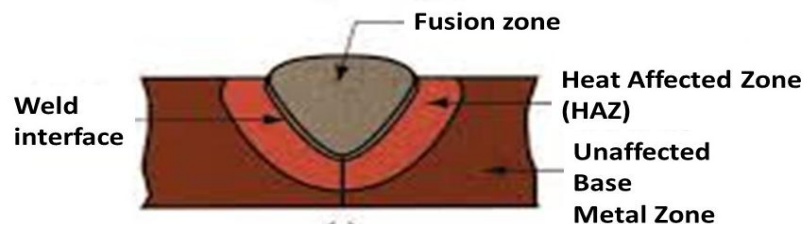


Figure 2: Schematic showing the regions of a heterogeneous weld



The after effect of a welded region of a carbon steel consists of transition parts from base metals to the filler metal. Those parts include the fusion zone, unmixed region, partially melted region, Heat Affected Zone and finally the unaffected base metal.<sup>[2]</sup> These regions are formed due to the excessive heat applied onto the carbon steel during the welding process.

The cycle of heat and cooling that occurs during welding affects the microstructure surface and composition of weld metal and the base metal. These causes other impacts to the weld metals and the parts involved as the heat change occurred influences the microstructure and also the compositions of the different parts that are present around the weld region. <sup>[4]</sup> The welded region undergoes microstructural and compositional heterogeneities therefore the welding behavior towards corrosion is tough to be estimated. The compositions of this part vary due to the mixture and due to this occurrence; a galvanic couple could be present. <sup>[5]</sup> The Table 1 shown below shows the compositional percentage of parent metal and the weld metal that is commonly used to repair pipeline defects.

Table 1: The compositional percentage (wt%) of parent metal and weld metal.

<b>Element</b>	<b>Al</b>	<b>As</b>	<b>C</b>	<b>Co</b>	<b>Cr</b>	<b>Cu</b>	<b>Fe</b>	<b>Mn</b>	<b>Mo</b>	<b>Nb</b>	<b>Ni</b>
Parent	0.037%	0.004%	0.21%	0.002%	0.049%	0.021%	98.3%	1.01%	0.010%	0.010%	0.024%
Weld	0.013%	0.005%	0.12%	0.002%	0.042%	0.046%	98.2%	1.07%	0.013%	0.005%	0.033%
<b>Element</b>	<b>P</b>	<b>S</b>	<b>Sb</b>	<b>Si</b>	<b>Sn</b>	<b>Ta</b>	<b>Ti</b>	<b>V</b>	<b>W</b>	<b>Zn</b>	<b>Zr</b>
Parent	0.013%	0.005%	0.007%	0.27%	0.004%	0.030%	0.003%	0.002%	0.016%	0.001	0.002%
Weld	0.012%	0.007%	0.008%	0.39%	0.004%	0.031%	0.002%	0.003%	0.014%	0.001%	0.003%

In an environment that contains high level of CO<sub>2</sub>, corrosion tends to happen at these regions and the PWC gives a bad damage to the pipelines. The compositional difference induced by the metallurgical change causes the potential difference and the galvanic couple to be formed. The galvanic reactions sometimes accelerate and sometimes retard the whole corrosion process to be occurring. When the corrosion occurs without the galvanic difference, then it is an intrinsic corrosion. However, when the combinations of galvanic and the intrinsic is to be occurring simultaneously, a focus of attack in a specific location of the weld region happens that leads to severe localized attack.<sup>[4]</sup>

The observation through the optical microscope can distinguish the different segments of the weld part by their grain size. Figure 7 shows the microstructural difference between the weld segments (parent metal, HAZ and weld metal).<sup>[28]</sup>

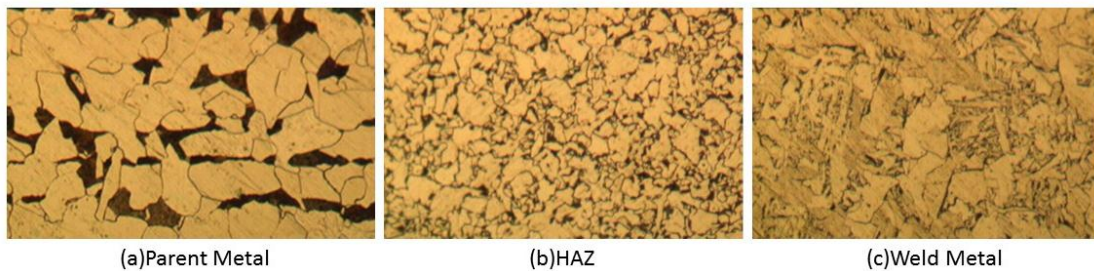


Figure 3 the microstructural difference between the weld segments under 100x magnification (a)parent metal (b) HAZ and (c)weld metal.

### **2.1.1 Parent metal**

Parent metal is the base metal in the weld region. It is far from the weld section. This part is not affected by the heat from the welding process. The metallurgical structure and the compositional characteristics of the parent metal remains unchanged during the welding process. <sup>[3]</sup>

### **2.1.2 Heat Affected Zone**

The Heat Affected Zone (HAZ) is the section of the weld segments that is affected due to high temperature. HAZ has experienced peak temperatures that could cause changes in the microstructure even at solid state but it is too low to be melted. Every point of the HAZ experiences different fusion line experiences due to the temperature and the cooling rate that is potential to alter the corrosion resistance of the affected metal. Even with many resources and researches throughout the years, it is still difficult in predicting the rate of preferential weld corrosion that would be experienced. The location of the corrosion, whether if it is on the HAZ or the weld fusion metal, could not be predicted. <sup>[2]</sup>

### **2.1.3 Weld Metal**

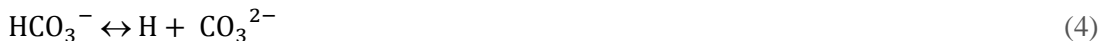
The weld metal is the result from the melting that forms the fusion between the filler metal and the base metal. This causes the characteristics of the metal part to be different form the base metal. <sup>19</sup> The part is situated in between the two parent metal structures.

## 2.2 Carbon Dioxide in Weld Corrosion

Welding region consists of Weld and HAZ is more prone to corrosion attack when under a corrosive environment. In the pipelines of the highly contented carbon dioxide environment, weld metal will act as a cathode whereas the parent metal undergoes oxidation as the anode. These conditions are initiated by the process of diffusion of CO<sub>2</sub> in water to produce the carbonate ions (CO<sub>3</sub><sup>2-</sup>). Later these ions react with the iron ion (Fe<sup>2+</sup>) from the parent metal to form Fe<sub>2</sub>CO<sub>3</sub> precipitation. This reaction does not take place abruptly but in a step by step sequence.<sup>[6]</sup> Firstly, under high pressure, Carbon dioxide gas dissolves in water and forms a “weak” carbonic acid through hydration by water.<sup>[8]</sup> The presence of carbon dioxide in solution leads to the formation of a weak carbonic acid (H<sub>2</sub>CO<sub>3</sub>) which drives CO<sub>2</sub> corrosion reactions as it is corrosive. This initiating step is shown by the reaction equation (1) and (2);



The weld corrosion is governed by several cathode reactions mainly on parent metal and anodic reaction on the weld metal. The cathode reactions include the reduction of carbonic acid into bicarbonate ions and the reduction of bicarbonate ions into carbonate ions as shown below by the equation (3) and (4):<sup>[7]</sup>



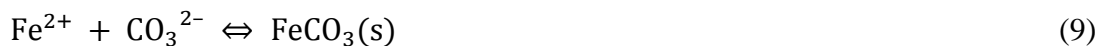
Solutions containing  $\text{H}_2\text{CO}_3$  are more corrosive to carbon steel. The  $\text{H}_2\text{CO}_3$  then acts onto the mild gaining an electron and releasing a proton to become hydrogen ion ( $\text{H}^+$ ). This reduction process results in Hydrogen (H) atoms and bicarbonate ions ( $\text{HCO}_3^-$ ). The formation of bicarbonate ion is showed by the equation (5) and the reduction of the hydrogen atom is shown by equation (6):<sup>[8-9]</sup>



The anodic reaction at the Parent Metal is however strongly pH-dependent. Equation (7) as per follows shows the reaction that occurs at the parent metal at low pH:



The insoluble corrosion product of reactions (3), (4), and (7) is iron carbonate ( $\text{FeCO}_3$ ) which forms by the reaction (8):



Reaction (3) and (4) produces hydrogen ions that forms electron at a fast rate. Reaction (5) and (6) produces hydrogen in the form of water. The direct reduction of  $\text{H}_2\text{CO}_3$  dominates at high partial pressures of  $\text{CO}_2$  and high pH values in the hydrocarbon pipelines.

Reduction of hydrogen ions dominates at low  $\text{CO}_2$  partial pressures and low pH. This process is determined by the amount of  $\text{CO}_2$  in the system. <sup>[9]</sup> Figure 4 shows the carbon dioxide corrosion mechanism that occurs on a metal surface.

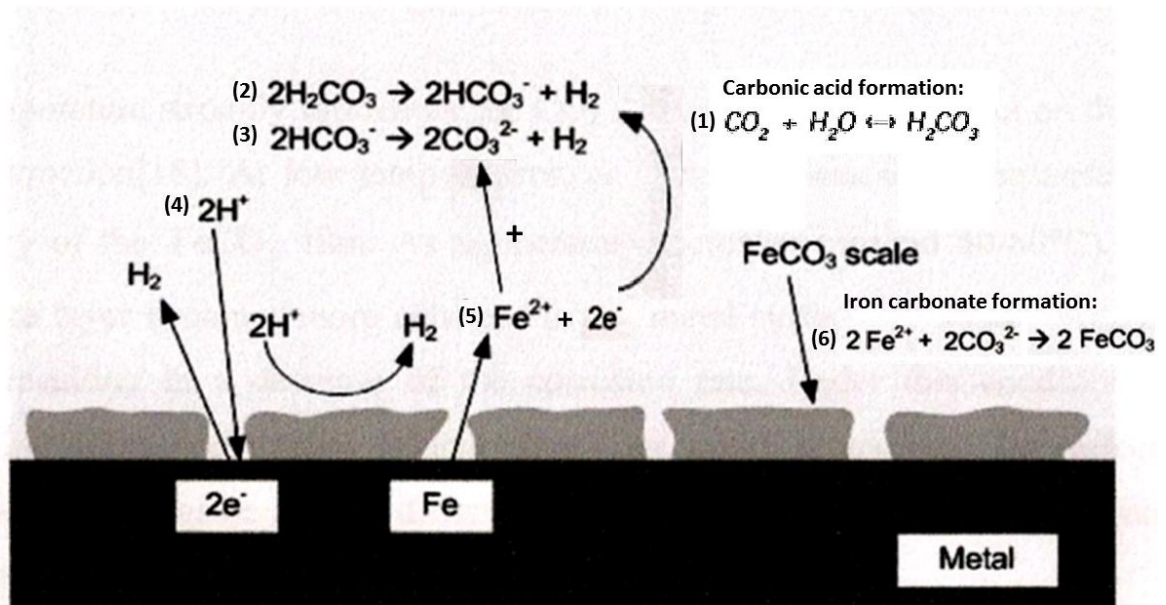


Figure 4: The Carbon dioxide corrosion mechanism.

Solubility of iron carbonate salt ( $FeCO_3$ ) formed may be exceeded and precipitation might set in. This is directly depending on the degree of super saturation and an increase in temperature of the whole environment. The iron carbonate precipitate may form a protective film on the HAZ and Weld Metal depending on the solution composition, pressure, and temperature of the entire system. The conditions that affects the  $CO_2$  corrosion in pipelines are varying conditions of pressure, temperature and pH.<sup>[10-13]</sup>

### 2.3 Acetic Acid in Carbon Dioxide Corrosion

Previous authors have investigated the effects of organic acid on CO<sub>2</sub> corrosion at the bottom of the line and their results have been used to predict the mechanism of corrosion occurring at the upper wall of the pipe [12, 13]. All the studies established that the presence of organic acid elevates the corrosion rate. Organic acid has the tendency to decrease the pH of the condensate and increase the solubility of iron (anodic reaction) due to the effect of un-dissociated (free) acetic acid on the cathode reaction of the corrosion process according to equation (10) and (11) [14].



The presence of acetic acid will also increase the solubility of iron in the condensed water thereby challenging the integrity of an iron carbonate films and increasing corrosion underneath the film [8]. Acetic acid will dissociate according to Equation 12, and supply more protons for the cathode reaction that supplies of H<sup>+</sup>. The increase in corrosion rate in the presence of acetic acid related to the formation of complex iron acetate Equation (13) instead of protective iron carbonate scale Equation (14).



Past studies show that CO<sub>2</sub> corrosion rate increased when HAc were added as acetic acid as it adds up H<sup>+</sup> concentration.

## 2.4 pH value influence

Lower pH value indicates higher acidity of the brine solution, which also means that the number of H<sup>+</sup> ions in the brine solution is also high. High concentration of H<sup>+</sup> ions would influence into an higher rate of corrosion.<sup>[3]</sup>

Concentration of H<sup>+</sup> can determine the distribution of the acetic in a solution. Concentration of the un-dissociated form of HAc and as acetate ion (Ac<sup>-</sup>) could also be predicted.<sup>[15]</sup>At high pH of 6.6, the CO<sub>2</sub> corrosion supposedly will not be affected since most of the HAc is present as acetate ion (Ac<sup>-</sup>). However, the presence of the weak acid will somehow disrupt the formation and protectiveness of FeCO<sub>3</sub> layer<sup>[8]</sup>

The precipitation by iron acetate (Fe(C<sub>2</sub>H<sub>3</sub>O<sub>2</sub>)<sub>2</sub>) does not occur due to its high solubility. <sup>[6]</sup> Based on past studies <sup>(9-11)</sup>, the major cause corrosion is the un-dissociated HAc and not the acetate ion (Ac<sup>-</sup>). Low pH has higher number of un-dissociated HAc.



## 2.5 Temperature influence on weld corrosion

Other studies have proven that the effect of temperature has a significant effect on the corrosion rate of the welded segment. Studies show that at higher temperature, the corrosion rate of a weld segment should increase. It has been reported that corrosion rate of pipeline weld segment could rise. However, the precipitation of protective layer onto the weld segment surface has also been reported to be sufficient at about temperatures above 75°C, based on corrosions occurring in the Top Line Corrosion (TLC).<sup>[6]</sup>

Increase in the temperature of the pipeline environment would cause a higher rate of corrosion due to the high CO<sub>2</sub> rate of reaction.<sup>[6]</sup> In contrary, when temperature decrease, high solubility of FeCO<sub>3</sub> does not form any protective layer. It is a prerequisite for initiating growth of FeCO<sub>3</sub> film that the solution must be supersaturated with regards to iron carbonate, implying that the saturation ratio (SR) of FeCO<sub>3</sub> must be >1. The saturation ratio is defined as;

$$SR = \frac{a_{Fe^{2+}} \cdot a_{(CO_3^{2-})}}{K_{sp}} \quad (15)$$

Where  $a_{Fe^{2+}}$  is the activity of iron ion,  $a_{(CO_3^{2-})}$  is the activity of carbonate ion and the  $K_{sp}$  being the solubility of FeCO<sub>3</sub>. The concentration-temperature curve for the solubility of FeCO<sub>3</sub> is inverse compared to most salts meaning the solubility increases with decreasing temperature. This means that the driving force for FeCO<sub>3</sub> precipitation, consequently SR, decreases with falling temperature. Another study proves that FeCO<sub>3</sub> has extremely slow precipitation kinetics at temperatures below 75°C. They claim that increased SR with high Fe<sup>2+</sup> and CO<sub>3</sub><sup>2+</sup> concentrations and high pH improves the adherence of such a film <sup>[5]</sup>.

It can be concluded that with high temperature (above 75°C), formation and precipitation of  $\text{FeCO}_3$  is more efficient compared to lower temperature. At lower temperatures, formation happens but the precipitation fails to occur due to high solubility of  $\text{FeCO}_3$ .

## **2.6 Intrinsic Corrosion**

The presence of  $\text{H}_2\text{O}$  and the oxygen could cause corrosion onto the surface of the metal sections without any galvanic difference. This type of corrosion is called the intrinsic corrosion or the self-passivation of the metal surface. Corrosion would occur due to the presence of  $\text{H}_2\text{O}$  and dissolved oxygen from air. Cathode reaction would form an oxide layer on the surface of the metal due to this corrosion.

## **2.7 Galvanic Corrosion**

Occurs between two different metals usually. In the context of PWC, galvanic corrosion occurs between the metal segments after the compositional alteration. The movement of electrons take place in the iron body and the corrosion take place on the anode, usually weld metal and the oxide layer formation usually takes place on the cathode, usually the parent metal.

## CHAPTER 3

### METHODOLOGY

#### 3.1 Project Work Flow

The work flow for this project is shown schematically in Figure 5.

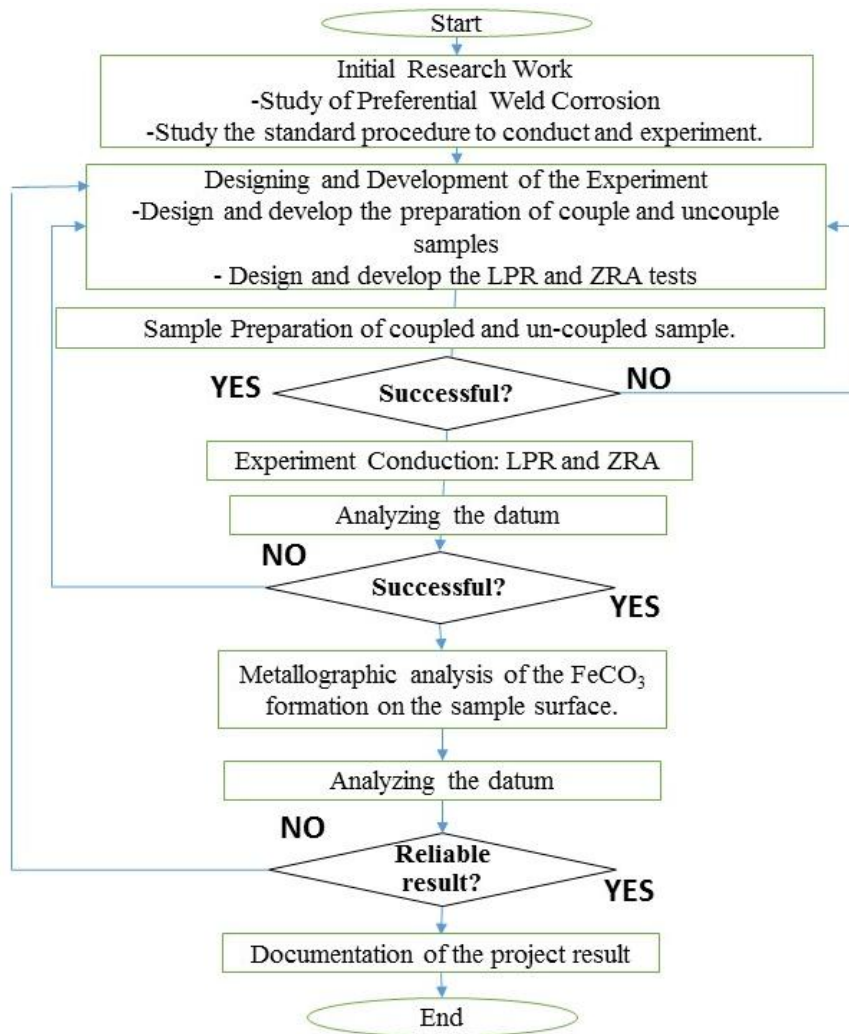


Figure 5: Project work flow for the entire 28 weeks.

### 3.2 Sample Preparation

There are six processes in sample preparation stage that has to be completed to prepare a working electrode for experiments. They are as following:

- i. Grinding and polishing.
- ii. Etching
- iii. Metallographic analysis
- iv. Sectioning process
- v. Cutting process
- vi. Cold mounting

A welded low carbon steel pipeline weld segment (API 5L X52) was obtained and was etched using 3% Nital solution as shown in Figure 6.



Figure 6: Grinded and polished weld segment has been etched using 3% Nital solution.

The weld region sample was further undergone the metallographic analysis using the Optical Microscope under the magnifications of 10x, 50x and 100 x in order to identify the microstructures.



Figure 7: The microstructural observation of weld segments using Optical Microscope (OM) with magnification 50x (a) parent metal (b) HAZ and (c) weld metal.

Microstructure characterization of the weld region was the most challenging task during sample preparation because each region must be precisely located before sectioning process otherwise they were not represented the welded joint of the pipelines. The colored lines between parent, HAZ, and weld metal is added after visual observation. Demarcation lines is drawn as shown in Figure 8.

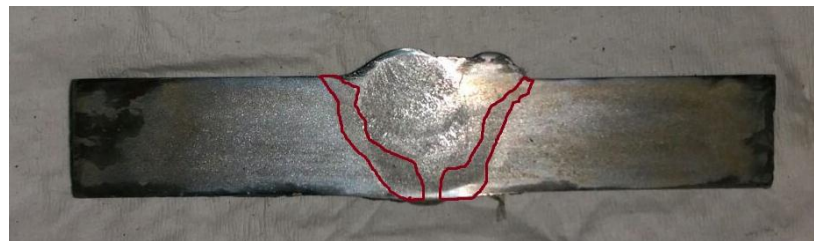


Figure 8: Demarcation line was constructed precisely in between the weld segments to have a better guideline when cutting.

The weld region sample was cut using the electrical discharge machine (EDM) wire cut into coupons in a ratio for parent metal, weld metal and HAZ respectively as to represent the field condition as shown in Figure 9.

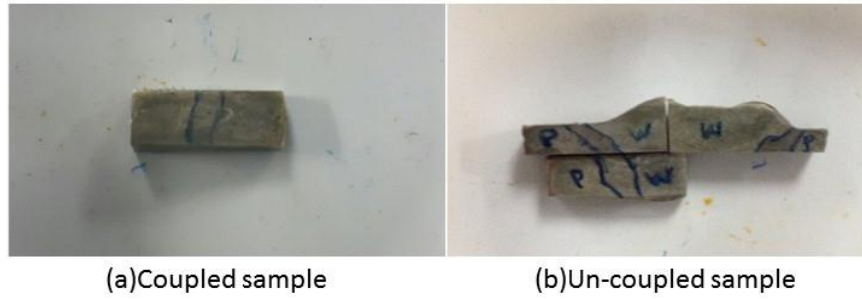


Figure 9: Samples obtained from the weld segment sectioning. (a) Coupled sample.  
(b) Un-coupled sample.

The Table 2 below shows the dimensions of the area of the weld segments .

Table 2: The ratio and the surface area of the sectioned weld samples

Experiment	Linear Polarization Resistance					
Sample type	Galvanic			Intrinsic		
Segments	Parent Metal	Heat Affected Zone	Weld Metal	Parent Metal	Heat Affected Zone	Weld Metal
Ratio	2	1	2	2	1	1
Surface Area (cm <sup>2</sup> )	0.5	0.28	0.29	0.76	0.42	0.50
Experiment	SEM					
Sample type	Galvanic			Intrinsic		
Segments	Parent Metal	Heat Affected Zone	Weld Metal	Parent Metal	Heat Affected Zone	Weld Metal
Ratio	3	1	1	3	3	2
Surface Area (cm <sup>2</sup> )	0.12	0.12	0.37	0.33	0.35	0.26

These segments were soldered with cooper wire for electrical connection and slotted through a 200 mm length, 0.3 mm diameter of P.V.C tube to provide support for the wire. The coupons were cast into epoxy resin in linear arrangement in a 30mm diameter mold to produce a working electrode. Most studies for preferential weld corrosion utilized this type of sample preparation because able to monitor the effect of galvanic within the weld region effectively. Electrodes were grinded with silicon carbide paper up to #600, then rinsed in acetone, blow-dried and placed in desiccators prior to use.

### 3.2.1 Galvanic Current (Coupled)

Figure 10 shows the design of the coupled weld sample.

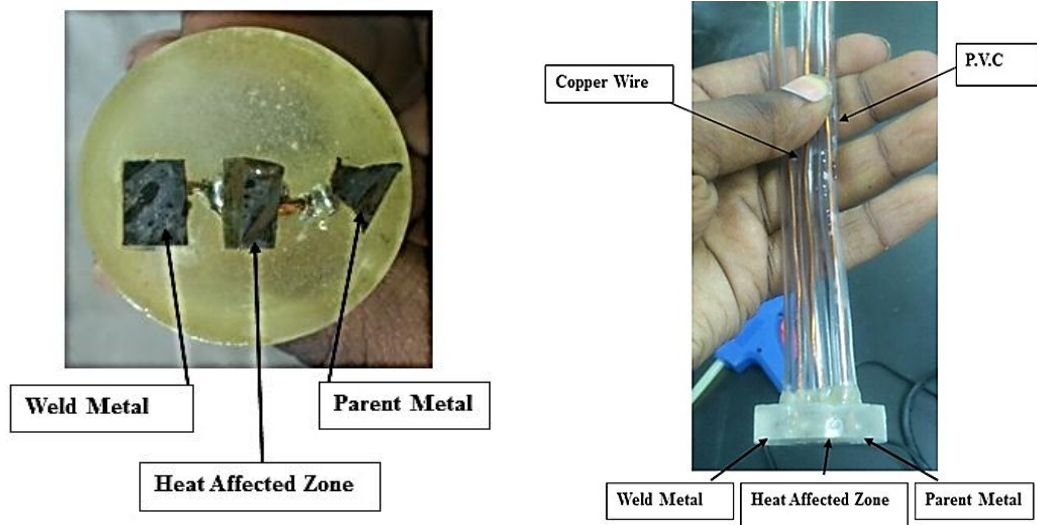


Figure 10: Coupled weld sample.

### 3.2.2 Intrinsic Current (Uncoupled)

Figure 11 shows the uncoupled weld sample.

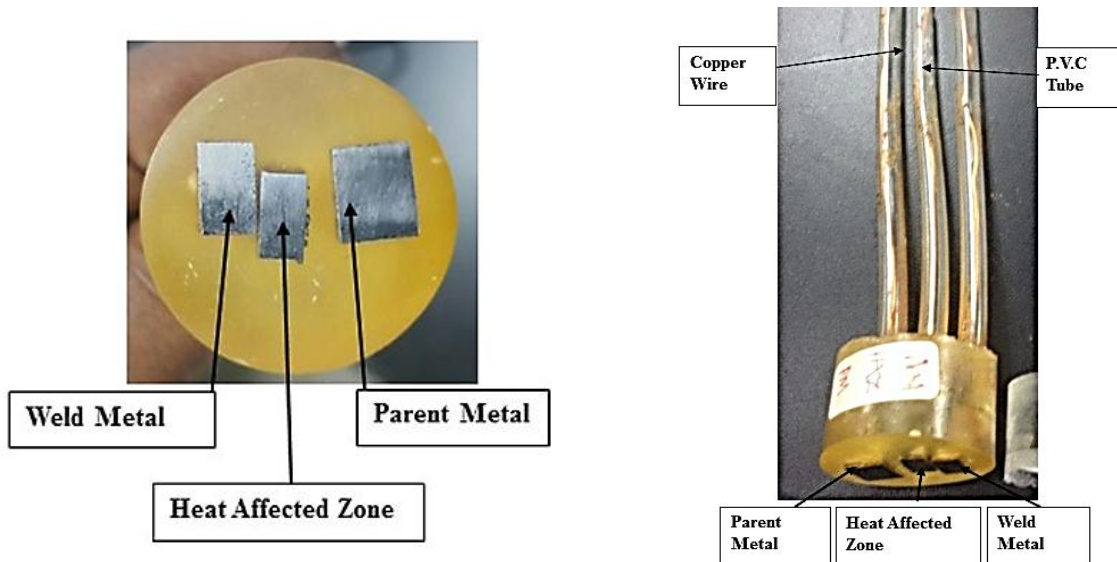


Figure 11: Un-coupled weld sample.

### 3.3 Experiment Execution

#### 3.4.1 Test Parameters

The Table 2 below shows the parameters of the experiments that was conducted. The parameters are fixed based on the real-life environment conditions of Top Line Corrosion (TLC). The brine is fixed to 3wt% NaCl and the Carbon dioxide (CO<sub>2</sub>) is continuously purged at 0.5 bar partial pressure. The temperature has been set to 80°C to simulate the environmental condition and for the precipitation of FeCO<sub>3</sub> to occur. The type of pipeline metal used is API 5L X52. The HAc concentration used is 1000 ppm based on previous studies. The pH is regulated to 4 and 6.6 to simulate both the existing conditions of the underwater environment based on recent papers. The test has been sorted into 4 parts labelled Test 1, Test 2, Test 3 and Test 4. Each test will undergo both intrinsic and galvanic tests.

Table 3: Test parameters designed for the conduction of the experiment.

Parameters	Test 1	Test 2	Test 3	Test 4
Brine	3 wt.% aqueous NaCl			
Carbon Steel	API 5L X52			
Partial pressure (bar)	0.53			
Concentration of acetic acid (ppm)	0	0	1000	1000
Temperature (°C)	80	80	80	80
pH	4	6.6	4	6.6



### **3.3.3 Experimental Setup**

The laboratory test will be set according to the determined operational parameters. The test solution used is NaCl solution of concentration 3wt%. The pH value is adjusted to 4.0 and 6.6 alternatively using 1M of HCl and 5M NaOH. The temperature of the brine solution will be heated to 80°C. Then, the tests were repeated for the different HAC concentrations with and without the presence of the inhibitor. The solution is purged with CO<sub>2</sub> at 1 bar to provide the environment of CO<sub>2</sub> corrosion. Each experiment was run with varying parameters for 24 hours and the data of the LPR was collected for both coupled and uncoupled sample segments. The data collected is then analyzed.

### 3.3.4 Experiment Procedures

Experiments procedures are as per described below:

1. Solution medium of sodium chloride 3% was prepared; 57g of sodium chloride was mixed into distilled water of 1.9 liter.
2. Working electrode, the Parent Metal was connected to WE1 connection, HAZ was connected to Z2 connection and Weld Metal was connected to Z3 connection.
3. The purging of the carbon dioxide gas was started and the solution was left for continuous purging for one until the carbon dioxide is saturated in the solution. The pH meter was used to determine whether the solution is saturated with carbon dioxide or not.
4. The glass cell was heated until the temperature of 80°C was obtained. The temperature is measured using a thermometer that will also be set up in the glass cell.
5. The pH of the solution was added with 1M HCl to attain a pH level of 4.0.
6. HAc of 0ppm was be added to the brine solution.
7. The chemicals and the coupled weld segment mounted in the epoxy was added into the solution, the data acquisition system will be accessed, the computer was connected to the ACM Instruments GalvoGill12 and the Core Running software.
8. The ACM Instruments ran and data was gathered automatically into the using ACM Instruments GalvoGill 12 that was connected to a data logging PC. The Zero Resistance Ammeter reading recorded down and the corrosion rate was calculated using the formula that will be discussed.
9. The test will be repeated for 1000ppm of HAc with the varying temperature and the pH set as per the suggested test matrix.

The currents flowing between segments will be measured using ZRA. Galvanic corrosion rate of the weld segment (coupled) and their intrinsic corrosion rates (uncoupled) will be recorded using same Linear Polarization Resistance (LPR) method. The total corrosion rate of each weld region will be obtained from the sum of the intrinsic and galvanic corrosion. The set-up of both the LPR and ZRA tests is set-up as per shown is Figure 12 below.

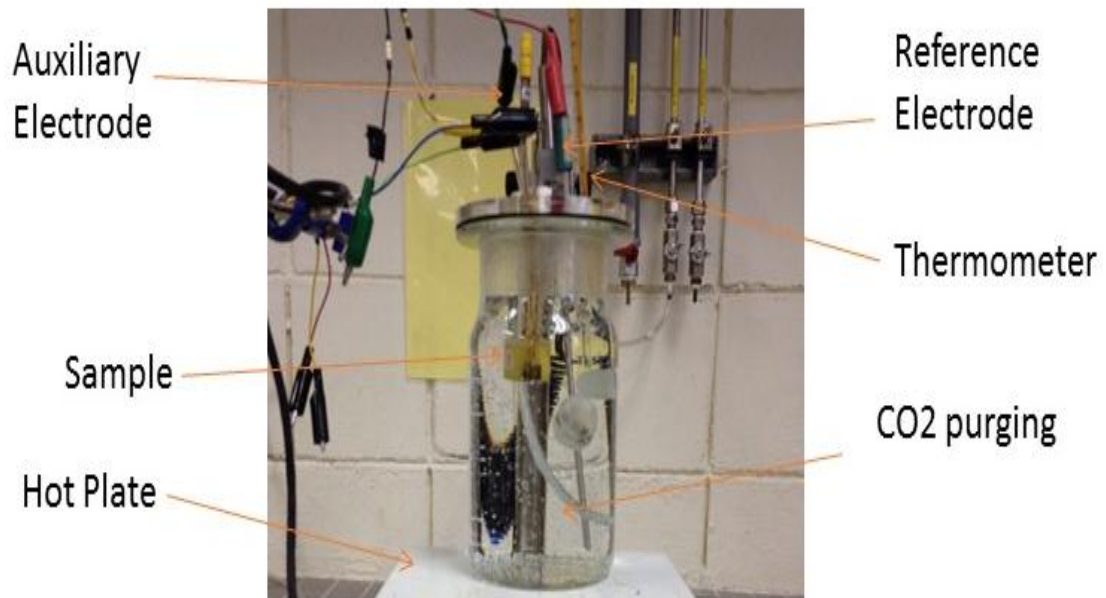
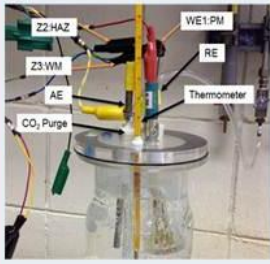
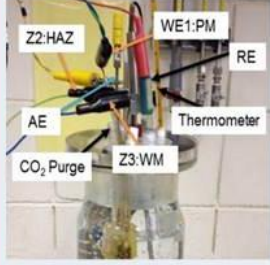


Figure 12: General experimental set up equipped with working electrode, reference electrode, auxiliary electrode, thermometer, CO2 bubbler, glass cell and hot plate for LPR and ZRA test.

### 3.3.5 Techniques of Evaluation

The Table 4 below shows the techniques that was used to obtain the results from the tests that were conducted.

Table 4: Techniques of evaluation that was used to obtain the results.

Sample	Techniques (4 Tests)	Results obtained	Glass-cell connection
Un-coupled	Linear Polarization Resistance (LPR)	Intrinsic Corrosion sweep (mm/yr)	
	Current & Voltage / time	Potential (mV) & Galvanic reading (mA/cm <sup>2</sup> )	
Coupled	Linear Polarization Resistance (LPR)	Galvanic Corrosion sweep (mm/yr)	
	Current & Voltage / time	Potential (mV) & Galvanic reading (mA/cm <sup>2</sup> )	
	Zero Resistance Ammeter (ZRA)	Current weld measurement (mA/cm <sup>2</sup> )	
	$I_{PM} + I_{HAZ} + I_{WM} = 0$		
Total corrosion	$CR_{Total} = CR_{Intrinsic} + CR_{Galvanic}$	Total corrosion rate (mm/yr)	

### 3.3.6 Linear Polarization Resistance (LPR)

LPR is a method using the linear approximation of the polarization behavior at potentials near the corrosion potential. Polarization resistance ( $R_p$ ) is given by Stern and Geary equation (16) :

$$R_p = \frac{B}{i_{\text{corr}}} = \frac{\Delta E}{\Delta I} \quad (16)$$

$$B = \frac{b_a b_c}{2.303(b_c b_a)} \quad (17)$$

The corrosion current is related to the corrosion rate from Faradays law:

$$CR \left( \frac{\text{mm}}{\text{yr}} \right) = \frac{(0.418)Z(i_{\text{corr}})}{n} \quad (18)$$

Where,

- CR = Corrosion rate (mm/yr)
- $i_{\text{corr}}$  = Corrosion current density
- Z = Atomic weight (g/ml)
- n = Electron number
- $b_a b_c$  = The slopes of the logarithmic local anodic and cathode polarization curves respectively
- $R_p$  = Resistance polarization (ohm)

Linear polarization resistance measurements were performed by measuring the corrosion potential of the exposed sample. Sweeping was done subsequently from -10 mV to + 10 mV with the sweep rate of 10 mV/min.

### 3.3.7 Galvanic Corrosion Test

The current flows from one to the other of two different conducting materials that is connected through an electrolyte is galvanic current [41,42]. Anodic member of the couple undergoes corrosion. Anodic member of couple is directly related to galvanic current by Faraday's law.

To measure the galvanic current of each weld region at specific time galvanic current density is performed. Circuit in Figure 13 shows the wire connection of galvanic experiment to the ZRA. Galvanic current test was conducted for the 4 coupled segments for 24 hours. Measurement data was recorded in mA/cm<sup>2</sup>. The schematic of weld segment connected to potentiostat is shown in Figure 13: Shows the connection between the electrodes and the Galvo Gill 12 for the ZRA test. The relation of current density of weld segment is as per shown in Equation (19). [6]

Galvanic currents between weld segments were recorded every 60 seconds with a ACM Instruments Galvo Gill 12 connected to a data logging PC. The current from the between the weld segments were recorded on two channels. The galvanic current recorded is evaluated in the following relationship; -

$$I_{PM} + I_{HAZ} + I_{WM} = 0 \quad (19)$$

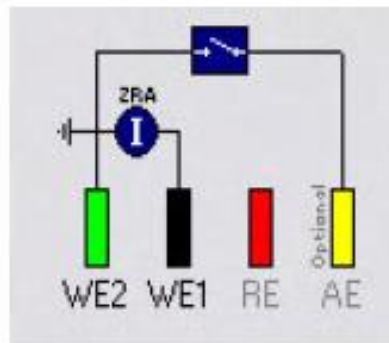


Figure 13: Shows the connection between the electrodes and the Galvo Gill 12 for the ZRA test

### 3.3.8 Intrinsic Corrosion

Intrinsic corrosion rate of the weld segments is by calculated using an uncoupled specimen electrode of RCE in turn and by LPR measurements. The reference electrode and the auxiliary electrode is used with LPR test. The potential of weld, HAZ and parent metal component was scanned 10 mV above and below its open circuit value, at a scan rate of 10 mV min<sup>-1</sup>. The polarization resistance, R<sub>p</sub>, was obtained from gradient of the potential/current graph. I<sub>CORR</sub>, was later calculated with equation (16); -

$$I_{CORR} = \frac{B}{R_P} \quad (16)$$

where B is a constant based on material and environment. LPR method is repeated over fixed period without changing the behavior of the material from its usual corroding condition.

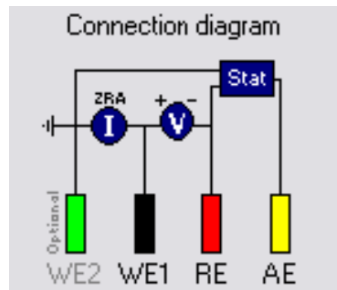


Figure 14: The connection between electrodes and Galvo Gill 12 for the LPR test.

### 3.3.9 Total Corrosion rate









The total corrosion rates of the three weld regions were found from the sum of their intrinsic corrosion rate and galvanic corrosion rate as per following: -

$$CR_{Total} = CR_{Intrinsic} + CR_{Galvanic} \quad (17)$$







### 3.3.10 Project Activities and Key Milestones




Table 5 below shows all the milestones that have been achieved during the completion of this report throughout the entire Final Year Project.

Table 5: The milestones that has been achieved throughout the completion of the Final Year Project.

No	Key Project Milestone	Expectation	Remarks	Milestone
	Literature Review	Week 2 - Week 5	Research on the Preferential Weld Corrosion and Carbon dioxide corrosion.	Week 4
	Literature Review	Week 2 - Week 5	Research on the effect of Acetic Acid on PWC under various parameters.	Week 5
	Extended Proposal Due	Week 7	Completion and the Submission of the Extended Proposal.	Week 7
	Methodology Construction	Week 6 - Week 14	Methodology is planned to have a vivid schedule and designing of the experiment.	Week 8
	Presentation	Week 11	Presentation of the Extended Proposal and the proposed methodology.	Week 11
	Experiment Design and Preparation of Weld Sample.	Week 8 - Week 16	Finalizing the experiment design based on the parameters to be tested. Etching with 3% Nital solution. Cutting using the EDM machine. Measuring the WM, HAZ and PM.	Week 15
	Evaluation	Week 15	Comment and evaluation by the supervisor.	Week 15
	Submission of Interim Report	Week 15	Submission of the Interim Report to the supervisor and the examiner.	Week 15



	Consultation with the Supervisor	Week 16 - Week 28	Consulting the supervisor regarding the sample preparation and obtain advise on the experiments to be done.	Week 16
	Conduction of the ZRA test.	Week 16 - Week 20	The experiment is conducted with the time period of 24 hours for each sample.  Readings are obtained using the ZRA machine.	Week 20
	Conduction of the LPR test.	Week 21 - Week 24	Readings are obtained using the LPR method for the intrinsic corrosion of the weld segment.	Week 24
 & 	Report Writing	Week 20 - Week 24	Report writing for both results obtained via ZRA and LPR methods.	Week 24
	Completion of Final Report	Week 25 - Week 26	Completion of the Final report Draft.	Week 24
	Report Writing Completion	Week 25 - Week 26	Report Writing completion and submission for improvement.	Week 25
	Submission of Final report draft.	Week 19 - Week 20	Progress work and preliminary result will be reported and discuss in the report for the submission to supervisor and coordinator. Reporting all progress and results that need to be analysed and discuss.	Week 25

	Dissertation Completion	Week 25	Dissertation is completed.	Week 25
	First Draft Presentation Slide	Week 27	First draft of presentation to be submitted for evaluation	Week 27
	Submission of Final Report	Week 28	Completed FYP report to be submitted to the examiner.	Week 28

### 3.3.11 Gantt Chart

The following table is showing the Gantt chart that has been constructed using the key milestones and the activities that has been done in completing the Study of Preferential Weld Corrosion in X52 Mild Steel with the presence of Acetic Acid. Table 6 shows the Gantt chart constructed for Final Year Project 1 and Table 7 shows the Gantt chart constructed for Final Year Project 2.

Table 6: Gantt chart of Final Year Project 1

Week	ALLOCATION WEEK	1	2	3	4	5	6	7	8	9	10	11	12	13	14	15
<b>Final Year Project Briefing</b>	1 DAY															
Topic Consolidation; Corrosion Inhibition of Preferential Weld Corrosion in the Presence of Acetic Acid	1 DAY															
Consultation with Supervisor;	THROUGHOUT 14 WEEKS															
<b>Topic Introduction</b>																
Background Study	1 DAY															
Objective	1 DAY															
Scope of Study	1 DAY															
<b>Literature Review</b>																
* What is Preferential weld Corrosion? * How does Carbon dioxide corrosion occur? * What is Acetic Acid? Research *What are the methods used to measure corrosion rate? * What are the factors affecting the corrosion rate? * Corrosion Stages of Acetic Acid. * Corrosion stages of Carbon Dioxide.	4 WEEK															
<b>Methodology</b>																
Deciding the parameters to be tested.	4 WEEK															
<b>Final Year Project Briefing 2</b>	1 DAY															
Designing the experimental procedure to be tested.	1 DAY															
Extended Proposal Due	1 DAY															
Design the Experiment: A glass cell test with varying parameters.	2 WEEKS															
Check the availability of tools and apparatus	2 WEEKS															
Methodology Construction 1) Conduct the experiment to study the relationship between the concentration of un-dissociated HAc and the Preferential Weld corrosion rate in varying environments. 2)Experiment to study the preferential weld corrosion behavior in the presence of inhibitor and HAc under varying conditions.	2 WEEKS															
Supervisor Verification	2 WEEKS															
<b>PROPOSAL DEFENCE</b>																
Presentation	1 DAY															
Submission	2 DAYS															
<b>EXPERIMENT</b>																
Planning	1 DAY															
Finalizing the Experimental Design: The parameters and the lab procedure is finalized.	1 DAY															
Material Preparation	2 DAYS															
Weld Sample Preparation	1 DAY															
<b>EVALUATION</b>																
Comment and evaluation by the Supervisor	1 DAY															
<b>COMPLETION</b>																
Submission of Report	1 DAY															

Table 7: Gantt chart of Final Year Project 2

Content	Allocation\ Week	1	2	3	4	5	6	7	8	9	10	11	12	13	14	
Consultation with Supervisor;	Throughout 14 weeks		▲9													
<b>Experiment Conduction : Glass Cell Test using ZRA tests.</b>																
Apparatus and Tools set up	4 Weeks															
Conduction of the Glass cell Test using the ZRA method.					▲10											
Cleaning Process																
Data Collection																
Analysing the datum collected.																
Verification of the collected datum																
Report Writing	1Day				▲11											
<b>Experiment Conduction : Glass Cell Test using LPR tests.</b>																
Apparatus and Tools set up	4 Weeks															
Conduction of the Glass cell Test using the LPR method.									▲12							
Cleaning Process																
Data Collection																
Analysing																
Verification of the collected datum																
Report Writing	1 Day								▲13							
<b>Completion of Final Report</b>	2 Weeks									▲14						
<b>Report Writing</b>	2 Weeks									▲15						
<b>Pre- SEDEX</b>	1 Day															
<b>FINAL REPORT</b>	1 Day															
Draft final Report	1 Week											▲16				
Disertation Completion	1 Day											▲17				
<b>Submission of Technical Report</b>	1 Day															
<b>Technical Presentation</b>																
First Draft Presentation Slide	1Week													▲18		
Mock Up resentation	1 Day															
Viva	1Day															
<b>COMPLETION</b>																
Submission of Interim Report	1Day															



## CHAPTER 4

### RESULTS & DISCUSSION

Table 8 shows the parameters of Test 1, Test 2, Test 3 and Test 4 that has been conducted in the basic conditions of 80°C, 3 wt.% NaCl, and 0.53 bar of CO<sub>2</sub> purging. The conditions of each test vary in terms of presence of HAc and pH value.

Table 9: Test parameters for 4 tests that has been conducted.

Parameters	Test 1	Test 2	Test 3	Test 4
Brine	3 wt.% aqueous NaCl purged with CO <sub>2</sub>			
CO <sub>2</sub> partial pressure	0.53 bar			
Temperature (°C)	80			
Carbon Steel	API 5L X52			
Concentration of HAc (ppm)	0	0	1000	1000
pH	4	6.6	4	6.6

The results obtained from this tests will be discussed in 3 segments; Intrinsic corrosion rate, galvanic corrosion rate and the metallographic analysis. Intrinsic corrosion rate is the corrosion rate of un-coupled sample and the galvanic corrosion rate is the corrosion rate recorded for the coupled sample.

#### 4.1 Intrinsic Corrosion Rates

Figure 15 shows the intrinsic corrosion of Test 1. The intrinsic corrosion rate of parent metal corrosion rate over time initially. On the 19<sup>th</sup> hour, the corrosion rate starts to decrease till the 24<sup>th</sup> hour. For HAZ, the corrosion rate decreases over 24 hours and as for the weld metal, corrosion rate is increasing steadily.

In Figure 16 for Test 2, it is observed that the corrosion rate for all three segments decreases in a constant pattern due to the continues growth of protective layer on the surface of the segments.

With addition of HAc in Test 3 as per shown in Figure 17, it appears that with lower pH, the pattern of corrosion rate is almost similar to the Test 2 which was conducted at pH 6.6 without HAc. The corrosion rate for all three segments decreases in a constant manner.

However, when the pH is increased in Test 4, the corrosion rate is identical to Test 2 and Test 3 until the 19<sup>th</sup> hour in Figure 18. At the 19<sup>th</sup> hour, the corrosion rate of weld metal and the parent metal rose significantly.

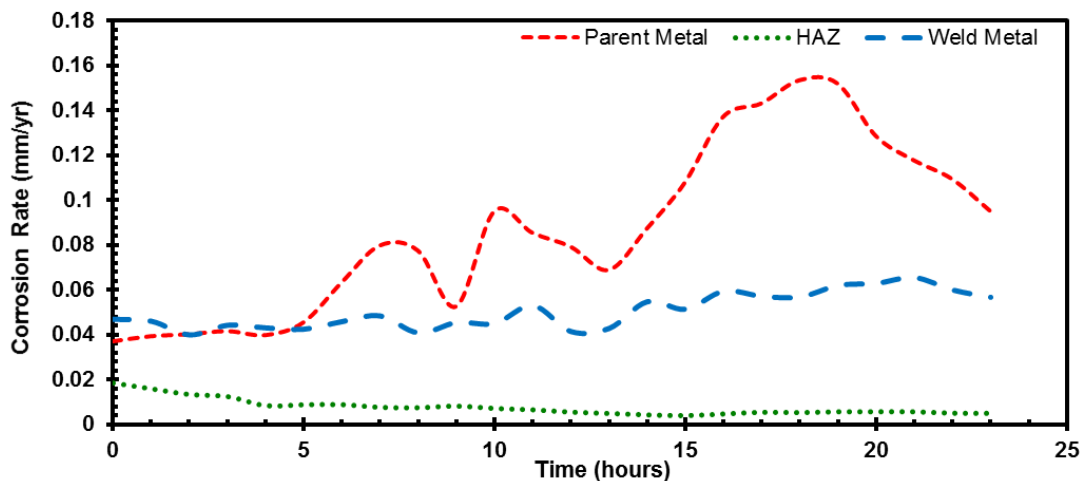


Figure 15: Test 1 intrinsic corrosion rate of uncoupled parent, HAZ, and weld metal with time at 80°C, 3 wt. % NaCl, 0 ppm HAc and pH 4.

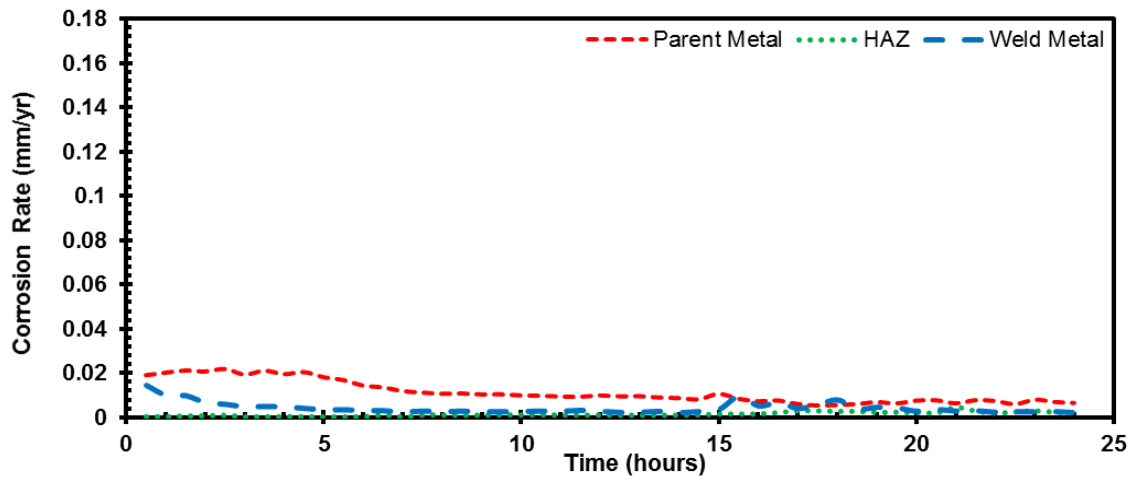


Figure 16: Test 2 intrinsic corrosion rate of uncoupled parent, HAZ, and weld metal with time at 80°C, 3 wt. % NaCl, 0 ppm HAc and pH 6.6.

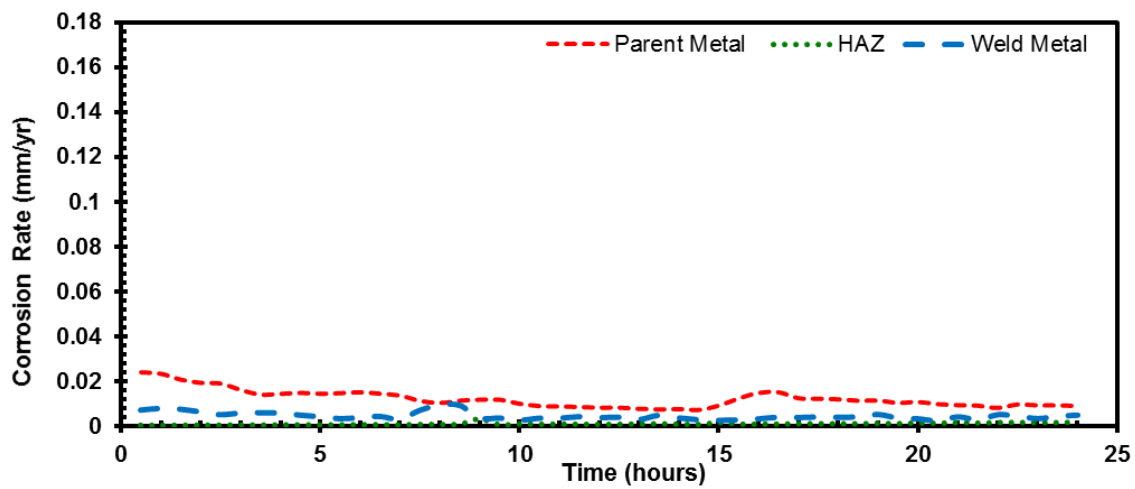


Figure 17: Test 3 intrinsic corrosion rate of uncoupled parent, HAZ, and weld metal with time at 80°C, 3 wt. % NaCl, 1000 ppm HAc and pH 4.



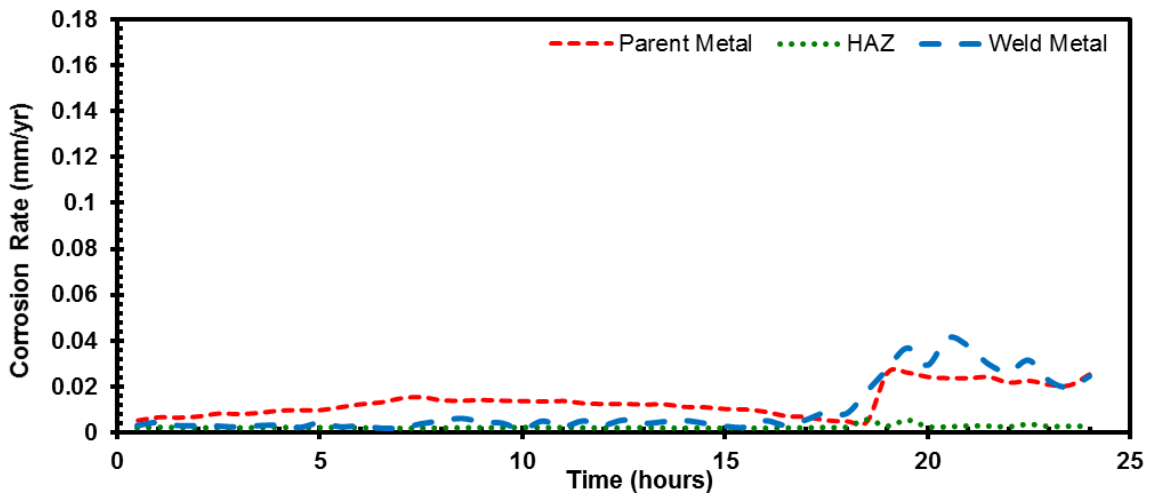


Figure 18: Test 4 intrinsic corrosion rate of uncoupled parent, HAZ, and weld metal with time at 80°C, 3 wt. % NaCl, 1000 ppm HAc and pH 6.6.

The intrinsic corrosion rate of metal segments as observed from the table below is very low that is below 0.1 mm/yr. However, amongst them, it can be observed that the parent metal undergoes higher corrosion rate throughout for all the tests. Following it would be the weld metal then the HAZ.

Table 10: The final intrinsic corrosion rate of weld segments

Segment	Corrosion Rate Calculated final average (24 h) [mm/yr]		
	Parent	HAZ	Weld
Test 1	0.10	<0.1	0.05
Test 2	0.01	<0.1	<0.1
Test 3	0.01	<0.1	<0.1
Test 4	0.02	<0.1	0.02

A bar chart was plotted with the final intrinsic corrosion rate readings of the parent metal, HAZ and the weld metals. Figure 19 shows the intrinsic corrosion rate of the 3 segments.

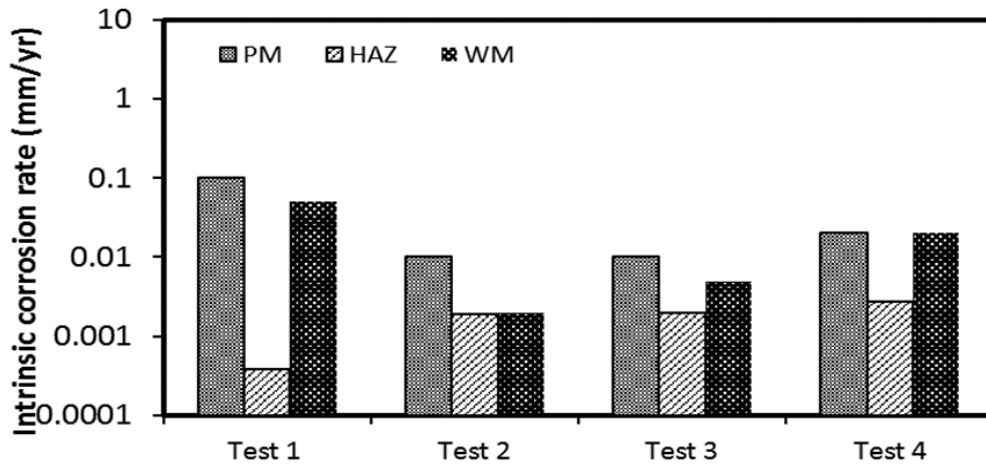


Figure 19: Intrinsic corrosion rate of parent, HAZ and weld.

The weld segment undergoes significant changes when it is reacted to the variation of pH values and the presence of Acetic Acid (HAc). For intrinsic corrosion in Figure 19, the parent metal is has high corrosion followed by weld metal and then the HAZ.

#### 4.2 Galvanic Corrosion Rates

Galvanic corrosion rate for Test 1 in Figure 20, show that with lower pH, the most active segment to undergo anodic reaction is the HAZ followed by weld metal and thirdly the parent metal. For Test 2 in Figure 21, the results show that the HAZ undergoes fluctuating corrosion rate for the 24 hours. The weld metal had high corrosion rate throughout leaving the parent metal being not reactive.

Test 3 in Figure 22 shows that the addition of HAc has elevated the corrosion rate of HAZ and weld metal from around the range of 2.5 mm/yr to the range of 5 mm/yr. When the pH is increased in Test 4, the Figure 23 show that the HAZ has fluctuating corrosion rate for the 24 hours. However, comparative to Test 2, the addition of HAc caused corrosion rate of HAZ to decrease while the corrosion rate of the weld metal has slightly risen.

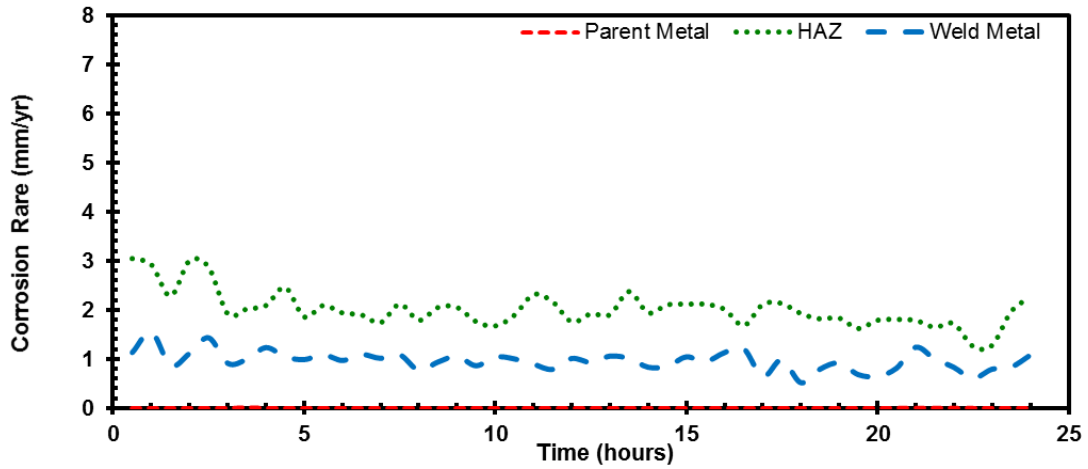


Figure 20: Test 1 galvanic corrosion rate of coupled parent, HAZ, and weld metal with time at 80°C, 3 wt. % NaCl, 0 ppm HAc and pH 4

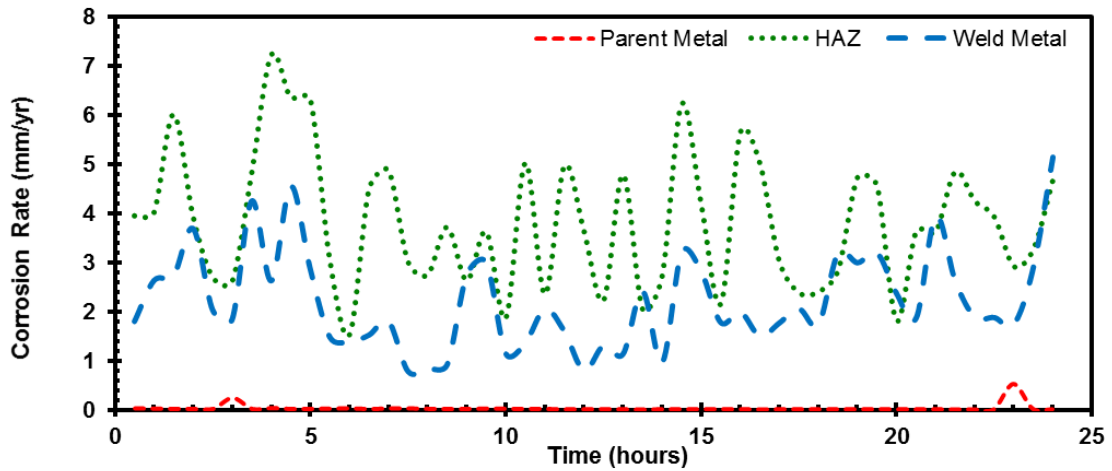


Figure 21: Test 2 galvanic corrosion rate of coupled parent, HAZ, and weld metal with time at 80°C, 3 wt. % NaCl, 0 ppm HAc and pH 6.6

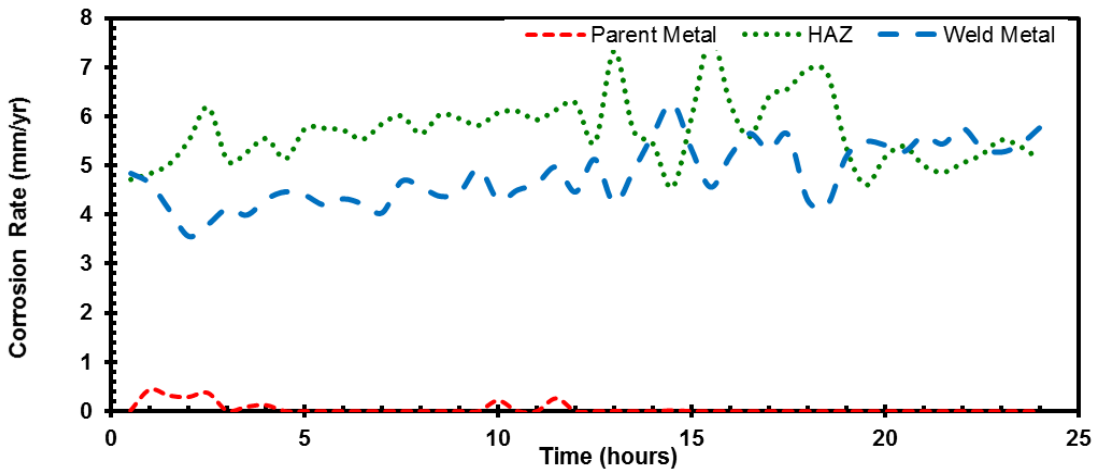


Figure 22: Test 3 galvanic corrosion rate of coupled parent, HAZ, and weld metal with time at 80°C, 3 wt. % NaCl, 1000 ppm HAc and pH 4.

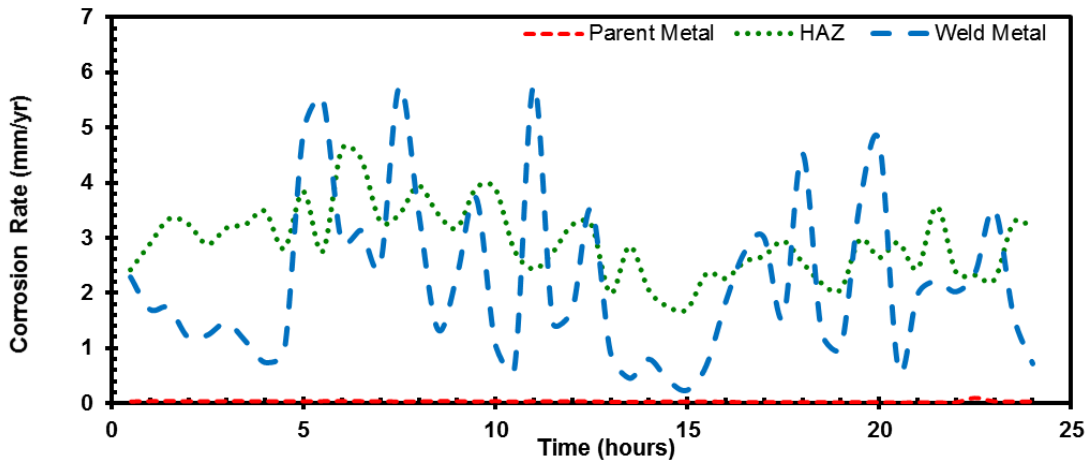


Figure 23: Test 4 galvanic corrosion rate of uncoupled parent, HAZ, and weld metal with time at 80°C, 3 wt. % NaCl, 1000 ppm HAc and pH 6.6.

Table 11 shows the final reading of galvanic corrosion rate of each weld segment. It shows that parent metal has approximately no corrosion occurring throughout the entire period excepting Test 2 and Test 4 whereby with the higher pH the corrosion rate seems noticeable. HAZ has higher corrosion rate with the presence of HAc. The HAZ corrosion

rate is even worse with both lower pH and HAc present. Weld metal shows the similar corrosion pattern with the HAZ segment.

Table 11: The galvanic corrosion rate of weld segments at initial point, final point and the average.

	Corrosion Rate <small>calculated final average (24 h)</small> [mm/yr]		
	Parent	HAZ	Weld
Test 1	<0.1	1.70	0.87
Test 2	0.12	3.80	2.72
Test 3	<0.1	5.25	5.51
Test 4	0.03	3.88	2.04

A bar chart was plotted with the final galvanic corrosion rate readings of the parent metal, HAZ and the weld metals. Figure 24 shows the galvanic corrosion rate of the 3 weld segments.

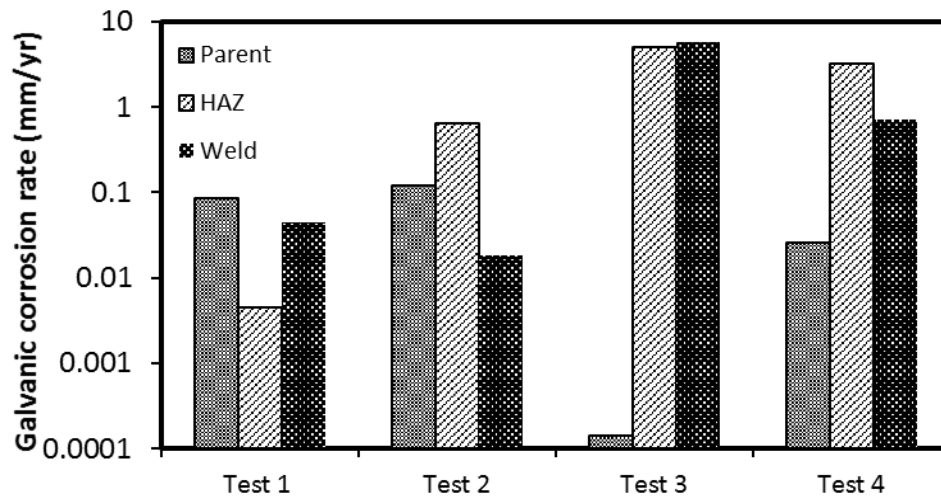


Figure 24: Galvanic corrosion of parent, HAZ and weld.

The weld segment undergoes significant changes when it is reacted to the variation of pH values and the presence of Acetic Acid (HAc). In Figure 24, the galvanic corrosion

the weld metal is observed to be the most reactive followed by the HAZ. The parent metal is left to be noble in the galvanic corrosion.

### 4.3 Total Corrosion Rate

A chart is plotted using the corrosion rate obtained for each of the weld segment. The total corrosion rate of the parent metal, HAZ, and the weld metal for the 4 tests are shown in Figure 25, Figure 26, and Figure 27 respectively.

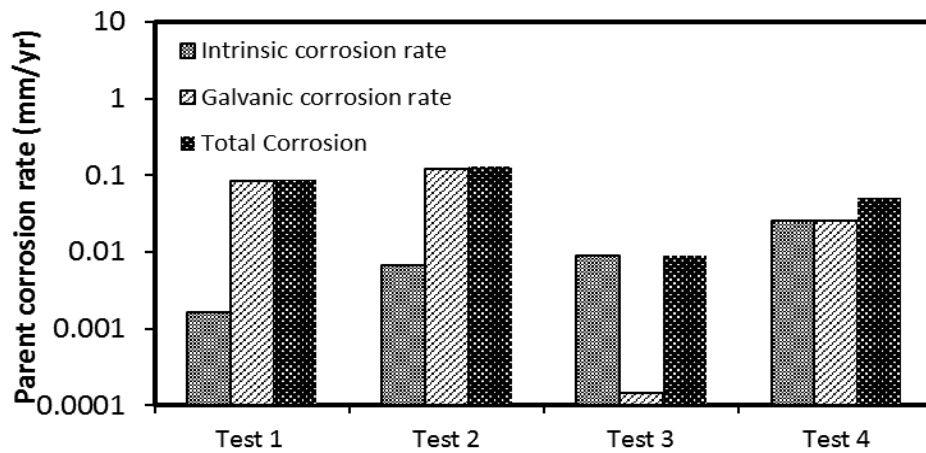


Figure 25: Total corrosion rate of parent metal compared to the intrinsic corrosion rate and galvanic corrosion rate.

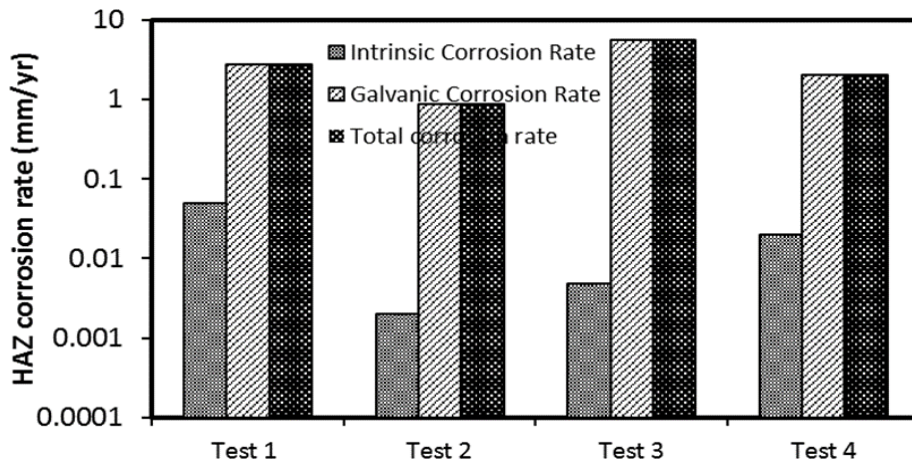


Figure 26: Total corrosion rate of HAZ metal compared to the intrinsic corrosion rate and galvanic corrosion rate.

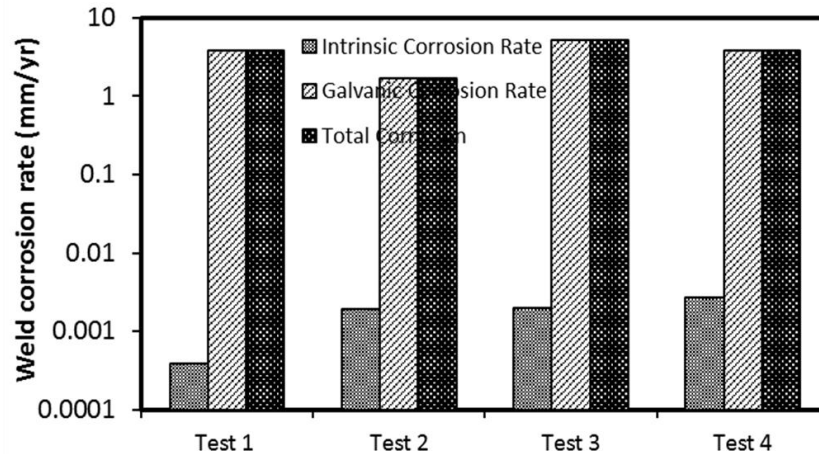


Figure 27: Total corrosion rate of weld metal compared to the intrinsic corrosion rate and galvanic corrosion rate.

The total corrosion rate of parent metal is shown in Figure 25. It appears that the total corrosion rate for the all four tests are below 0.1 mm/yr. The total corrosion rate of the parent metal is highly depending on the intrinsic corrosion undergone by the metal segment, since the galvanic corrosion rate is negligible.

Figure 26 shows the bar chart for the total corrosion rate of HAZ metal segment. Test 3 seems to be undergoing the highest corrosion rate compared to the other tests. The test with the least total corrosion rate will be Test 2. The corrosion rate of HAZ metal segment is due to the high galvanic corrosion it went through.

Figure 27 shows the bar chart for total corrosion rate of the weld metal segment. It appears that the pattern of total corrosion rate of weld metal segment is identical to the pattern on the HAZ segment. This may be due to the high galvanic corrosion these segments went through. The highest total corrosion rate is for Test 3 and the lowest total corrosion rate is for Test 2.

### 4.3.1 Effect of HAc presence

Parent metal's total corrosion, based on Figure 25 has a significant difference with and without the presence of HAc. The total corrosion rate of parent metal is higher without the presence of HAc. Addition of HAc mitigates the corrosion rates at both Test 3 and Test 4 regardless of the pH. Comparing Test 1 and Test 3 which is at pH 4, the total corrosion rate for Test 3 with the presence of HAc is even higher. This could be predicted as a protective layer is being formed on the parent metal surface with the presence of high concentration HAc. Similar pattern can be observed when comparing Test 2 and Test 4 which has been conducted at pH 6.6. The total corrosion rate of Test 4 that has been conducted with 1000ppm HAc is lower compared to Test 2 that was conducted without HAc.

Total corrosion rate of HAZ is shown in Figure 26. Addition of HAc shows vast increment in the total corrosion which is as predicted initially. At pH 4, comparing Test 1 and Test 3, it has been observed that the corrosion rate is higher. This could be justified as with the presence of HAc in Test 3, the formation of  $\text{FeCO}_3$  layer is more challenging when comparing Test 1 that was conducted without HAc. The high concentration of HAc causes soluble iron acetate,  $\text{Fe}(\text{CH}_3\text{COOH})_2$  to be formed. Due to its high solubility, the iron acetate fails to precipitate. The formation of  $\text{FeCO}_3$  is disrupted due to this reaction. No protective layer is present on the surface of the HAZ causing it to undergo high corrosion in Test 3. The pattern is also observed with higher pH for Test 2 and Test 4. Test 4 which has the presence of HAc has higher total corrosion rate when compared with Test 2 that does not have the presence of the weak acid.

Based on Figure 27, the total corrosion of weld metal is from its galvanic corrosion rate. The total corrosion rate of weld metal is similar to the total corrosion rate pattern of the HAZ. Addition of HAc in Test 3 shows vast increment in the galvanic corrosion when compared with Test 1. High concentration of HAc prevented the protective layer formation causing the weld metal surface to be exposed to anodic reaction. Test 4 which has HAc



present also faces similar reaction when compared with Test 2. The presence of HAc causes the corrosion rate of weld metal is to be higher regardless of the pH value.

#### **4.3.2 Effect of pH value.**

Parent metal total corrosion rate, in Figure 25 has a significant impact with the pH variation. Comparing Test 1 and Test 2 conducted without HAc present, Test 1 that has been conducted at pH 4 has lower total corrosion rate when compared with Test 2 that has been conducted at pH 6.6. When Test 3 and Test 4 that was conducted with the presence of HAc is observed, it appears that Test 4(pH 6.6) has higher corrosion rate compared with Test 3(pH 4). This is contrary to the behavior of the other weld segments or as per prediction. A possible protective layer could be forming on the parent metal with lower pH regardless of the presence of HAc.

Total corrosion rate of HAZ is shown in Figure 26. Test 1 and Test 2 was compared. These tests, without the presence of HAc shows that at lower pH the corrosion rate is the highest. When comparing Test 3 and Test 4, that is conducted with 1000ppm HAc, Test 3 that is with the pH 4 shows higher total corrosion rate when compared with Test 4. This is justified as at lower pH, the concentration of  $H^+$  is even higher. The dissolution of iron occurs (anodic reaction). Another justification is, at higher pH, the precipitation of  $FeCO_3$  much more favorable. The formation of the carbonate layer may have decreased the corrosion rate in both Test 2 and Test 4.

Based on Figure 27, the total corrosion of weld metal is similar to the total corrosion rate pattern of the HAZ. Test 4 and Test 2 that was conducted at pH 6 has lower total corrosion rate. Test 1 and Test 3 that was conducted at pH 4 has higher total corrosion rate. Test 3 has the highest total corrosion rate. Precipitation of  $FeCO_3$  is predicted to be occurring on the weld metal of Test 4 and Test 2 since at higher pH the solubility of the iron carbonate decreases.

#### 4.4 Surface Morphology

The specimen surfaces were scanned by SEM after the LPR test. The surface morphologies of the parent, the HAZ, and the weld metal surface after the 4 tests are shown in Figure 28, Figure 29, Figure 30 and Figure 31.

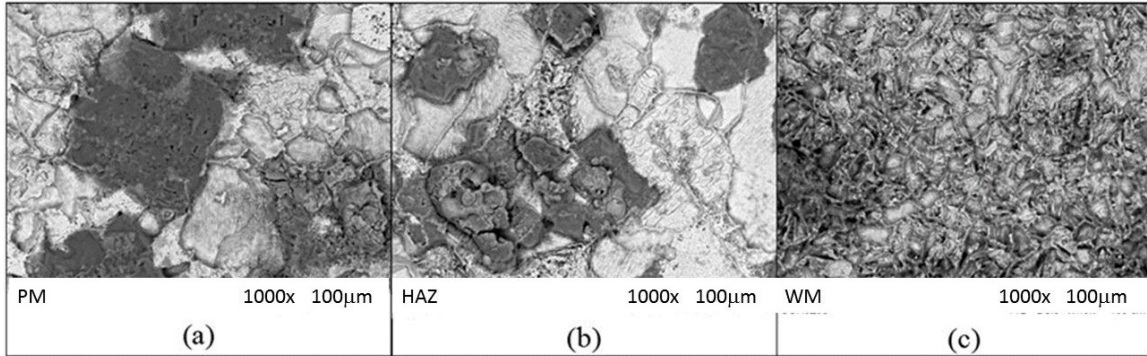


Figure 28: Test 1 coupled specimen surface morphology of (a) parent steel, (b) HAZ and (c) weld metal after 24 hours LPR test.

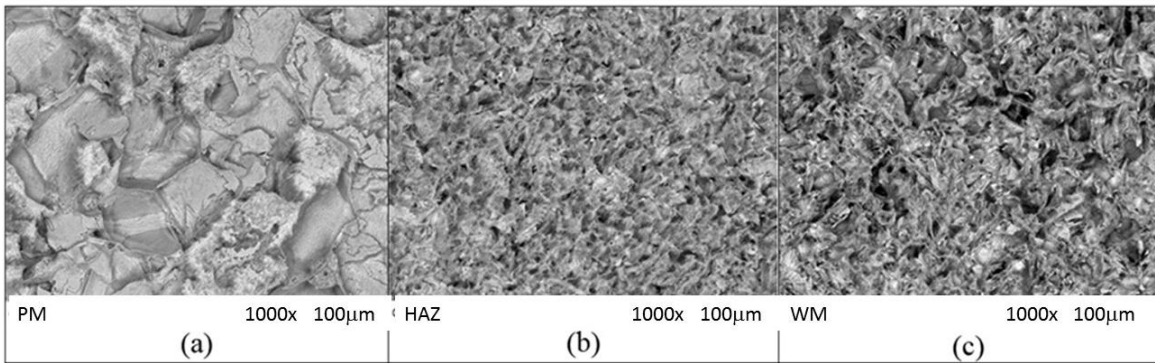


Figure 29: Test 2 coupled specimen surface morphology of (a) parent steel, (b) HAZ and (c) weld metal after 24 hours LPR test.

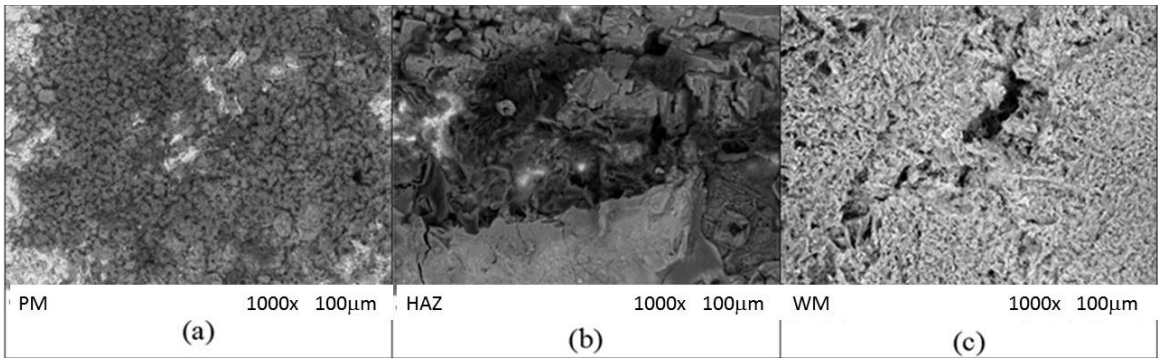


Figure 30: Test 3 coupled specimen surface morphology of (a) parent steel, (b) HAZ and (c) weld metal after 24 hours LPR test.

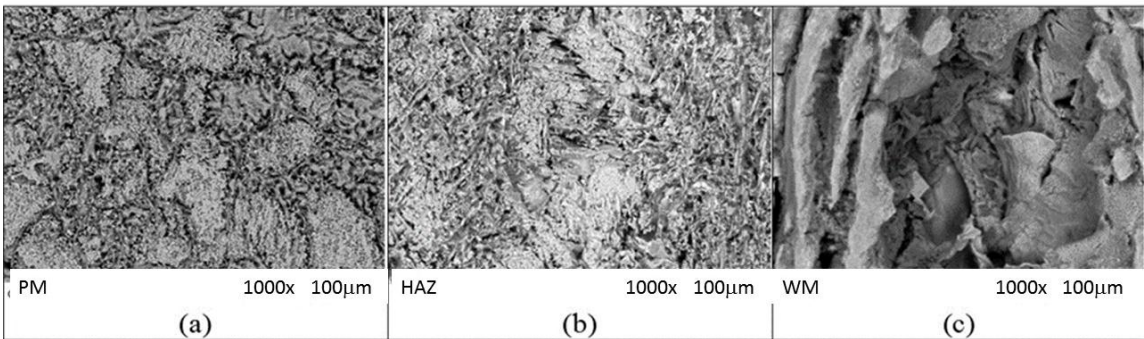


Figure 31: Test 4 coupled specimen surface morphology of (a) parent steel, (b) HAZ and (c) weld metal after 24 hours LPR test.

Evidence of localized attack on coupled specimen of Test 1, Test 3 and Test 4 was detected. Test 1 shows corroded region on the parent metal and the HAZ. Weld metal is covered with a layer of film. Test 2 surface scanning shows that a film layer has covered throughout all three parent metal, weld metal and the HAZ. HAZ and weld metal of Test 3 shows corroded surface. A thin layer of film happens to be appearing on the surface of the parent metal. Weld metal of Test 4 coupled specimen indicates corroded surface. However parent metal and HAZ is covered by a layer of film.

The Figure 32 below shows the cross section of the  $\text{FeCO}_3$  layer thickness on coupled sample and the EDX analysis under the SEM test for conditions specified for Test 2.

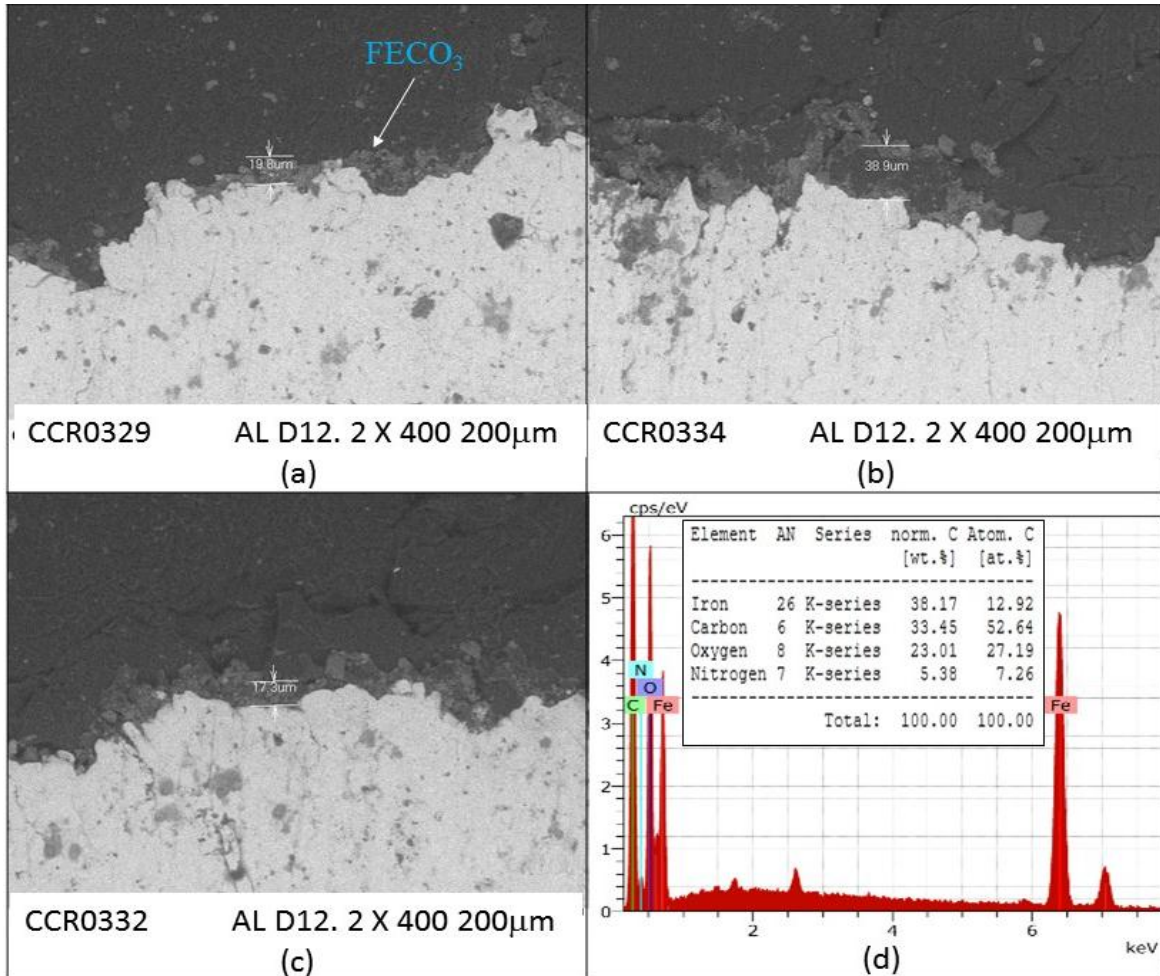


Figure 32: SEM micrograph showing the cross section of the  $\text{FeCO}_3$  layer formed coupled sample under Test 2 experimental conditions. (a) parent metal surface;(b) HAZ surface;(c) weld metal surface;(d) EDX results.

Based on Figure 32, the Test 2 coupled samples show that the oxide formation of the HAZ is the thickest amongst the rest. The following would be the parent metal followed by the weld metal. This observation infers the high corrosion rate of the weld metal throughout the Test 2 conduction with pH 6. However, the formation of the film layer on the parent metal and HAZ is not uniform. There are only spots of  $\text{FeCO}_3$  that could be



observed through the SEM result. The un-uniform formation of film layer may be the cause that the HAZ has a high total corrosion for Test 2 as well.

Figure 33 below shows the cross section of the  $\text{FeCO}_3$  layer thickness on coupled sample and the EDX analysis under the SEM test for conditions specified for Test 4.

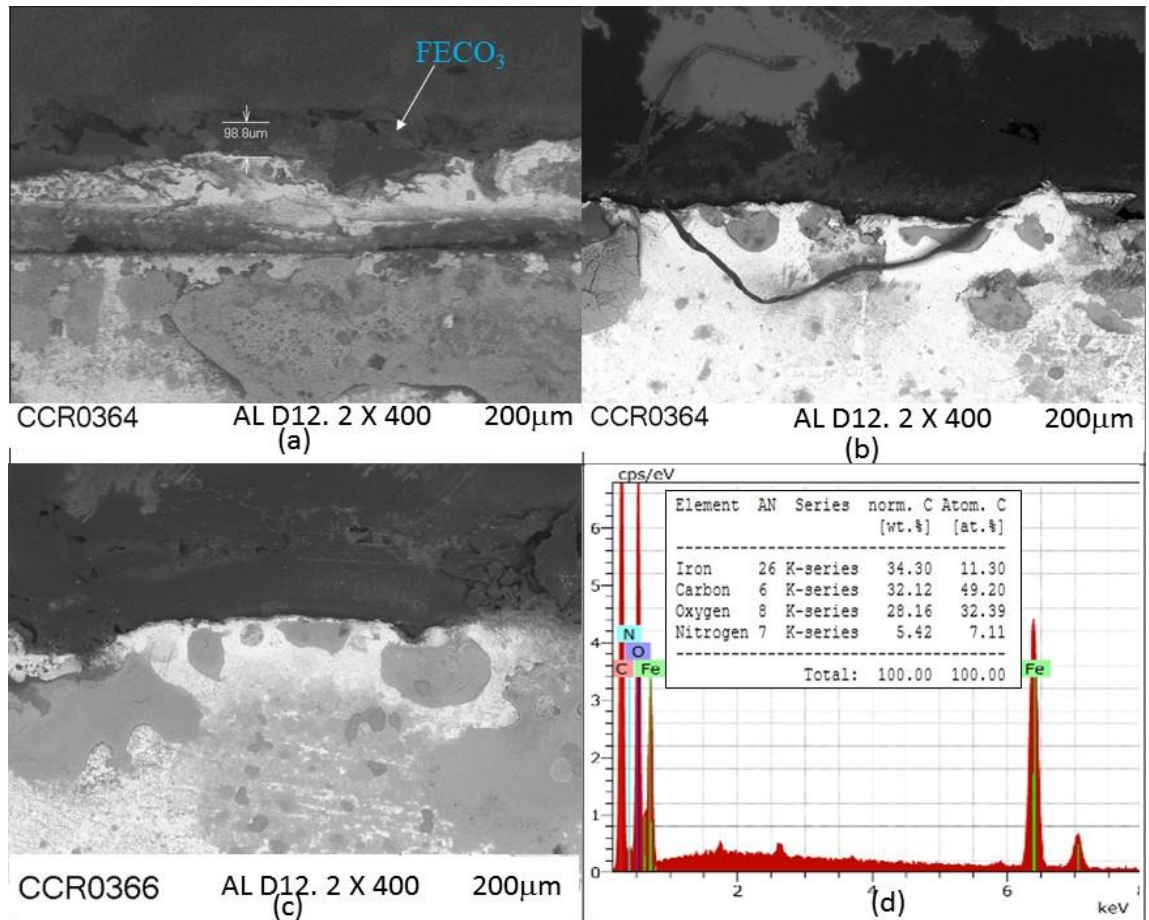


Figure 33: SEM micrograph showing the cross section of the  $\text{FeCO}_3$  layer formed coupled sample under Test 4 experimental conditions. (a) parent metal surface;(b) HAZ surface;(c) weld metal surface;(d) EDX results.

Based on Figure 33, the Test 4 coupled samples show that only parent metal has been covered with  $\text{FeCO}_3$  layer. This layer of protection is not sufficient since it is not uniformly grown on the surface. The HAZ and the weld metal surface does not have any carbonate formation. It is exposed to the anodic reaction to occur.

## CHAPTER 5

### CONCLUSION & RECOMMENDATION

#### 5.1 Conclusion

The presence of weak acids such as Acetic Acid (HAc) influences the formation of  $\text{FeCO}_3$  protective layer. The pH of the environment also influences the reaction HAc.

The following can be concluded from the LPR tests and the surface morphology that has been conducted;

1. Without the presence of HAc, increasing the pH value from 4 to 6.6 causes 66% of total corrosion rate increment.
2. With the presence of 1000ppm HAc, increasing the pH value from 4 to 6.6 causes total corrosion rate to increase by 62%.
3. At constant pH 4, addition of 1000 ppm HAc increases the total corrosion rate by 55%.
4. At constant pH 6.6, addition of 1000 ppm HAc increases the total corrosion rate by 50 %.
5. Under constant pH 6.6, a thin uniform layer of  $\text{FeCO}_3$  with the absence of HAc.
6. Presence of HAc at pH 6.6 forms spots of thick  $\text{FeCO}_3$  on parent metal only.
7. Total corrosion rate is the highest with 1000ppm HAc at low pH of 4.
8. The corrosion rate of Test 3 and Test 4 is higher when compared with Test 1 and Test 2 results that were conducted without HAc for both HAZ and weld metal.

## 5.2 Recommendation

Further investigations need to be done to study the effect of HAc and the pH influence onto the weld corrosion. The test must be done. The following improvements need to be taken into account in the future tests;

1. Identify the formation of the protective film that has formed on the surface of the parent metal under low pH with HAc present.
2. Conduction of tests to investigate the HAc under varying temperature of 25°C and 60°C.
3. Investigate the formation of  $\text{FeCO}_3$  layer under different concentrations of HAc such as 85 ppm and 850 ppm under constant pH of 6.6.

## REFERENCING

1. R. Barker, X. Hu, A. Neville and S. Cushnaghan, 'Assessment of Preferential Weld Corrosion of Carbon Steel Pipework in CO<sub>2</sub>-Saturated Flow-Induced Corrosion Environments', *Corrosion*, vol. 69, no. 11, pp. 1132-1143, 2013.
2. Corrosion of Weldments, D. Olson, *Welding, brazing, and soldering*. [Metals Park, OH]: ASM International, 1993.p 1065-1069
3. Twi-global.com, 'FAQ: What are the causes of and solutions to the preferential weld corrosion in C-Mn steels?', 2015. [Online]. Available: <http://www.twi-global.com/technical-knowledge/faqs/material-faqs/faq-what-are-the-causes-of-and-solutions-to-the-preferential-weld-corrosion-in-c-mn-steels/>. [Accessed: 07- Nov- 2015].
4. D. Queen, L. Chi-Ming, J. Palmer and E. Gulbrandsen, 'Guidelines For The Prevention, Control And Monitoring Of Preferential Weld Corrosion Of Ferritic Steels In Wet Hydrocarbon Production Systems Containing CO<sub>2</sub>', *Society of Petroleum Engineers*, 2004.
5. C. Lee, P. Woollin and S. Bond, 'Preferential weld corrosion: Effects of weldment microstructure and composition', *Proc. of Corrosion NACE International*, 2005.
6. K. George and S. Nestic, 'Investigation of Carbon Dioxide Corrosion of Mild Steel in the presence of Acetic Acid', *NACE International*, vol., 2007.
7. K. Alawadhi and M. Robinson, 'Preferential weld corrosion of X65 pipeline steel in flowing brines containing carbon dioxide', *Corrosion Engineering, Science and Technology*, vol. 46, no. 4, pp. 318-329, 2011.
8. C. de Waard, U. Lotz and D. Milliams, 'Predictive Model for CO<sub>2</sub> Corrosion Engineering in Wet Natural Gas Pipelines', *Corrosion*, vol. 47, no. 12, pp. 976-985, 1991.
9. S. Nestic, J. Postlethwaite and S. Olsen, 'An Electrochemical Model for Prediction of Corrosion of Mild Steel in Aqueous Carbon Dioxide Solutions', *Corrosion*, vol. 52, no. 4, pp. 280-294, 1996.



10. S. Nes̃ic', G.T. Solvi, J. Enerhaug, *Corrosion* 51, 10 (1995): p. 773.
11. S. Nes̃ic', J. Postlethwaite, S. Olsen, *Corros. Sci.* 52, 4 (1996): p. 280.
12. S. Nes̃ic', B.F.M. Pots, J. Postlethwaite, N. Thevenot, *J. Corros. Sci. Eng.* 1, paper no. 3 (1995).
13. S. Nes̃ic', M. Nordsveen, R. Nyborg, A. Stangeland, "A Mechanistic Model for CO<sub>2</sub> Corrosion with Protective Iron Carbonate Films," *CORROSION/2001*, paper no. 01040 (Houston TX: NACE, 2001).
14. B. Hedges, L. McVeigh, "The Role of Acetate in CO<sub>2</sub> Corrosion: The Double Whammy," *CORROSION/1999*, paper no. 21 (Houston TX: NACE, 1999).
15. J.-L. Crolet, N. Thevenot, A. Dugstad, "Role of Free Acetic Acid on the CO<sub>2</sub> Corrosion of Steels," *CORROSION/1999*, paper no. 24 (Houston, TX: NACE International, 1999).
16. E. Gulbrandsen and A. Dugstad, 'Corrosion Loop Studies of Preferential Weld Corrosion and Its Inhibition in CO<sub>2</sub> Environments', *Institute for Energy Technology*, 2007.
17. E. Gulbrandsen and K. Bilkova, 'Solution Chemistry Effects on Corrosion of Carbon Steels in Presence of CO<sub>2</sub> and Acetic Acid', *NACE*, 2006.
18. Corrosion Inhibitors', *CANMET Materials Technology Laboratory Ottawa, Ontario, Canada*, vol. 59, pp. 15-17, 2015.
19. 2015. [Online]. Available: <http://corrosioncost.com/>. [Accessed: 29- Oct- 2015].
20. J. Speight, 'The chemistry and technology of petroleum'. New York: Marcel Dekker, 1999.
21. M. Garcia, L. et al., 'Correlation Between Oil Composition and Paraffin Inhibitors Activity', *SPE Annual Technical Conference and Exhibition*, 1998.
22. P. Singh, 'Gel deposition of cold surfaces', Ph.D, University of Michigan., 2000.
23. M. Nordsveen, et al., 'A Mechanistic Model for Carbon Dioxide Corrosion of Mild Steel in the Presence of Protective Iron Carbonate Films—Part 1: Theory and Verification', *Corrosion*, vol. 59, no. 5, pp. 443-456, 2003.

24. S. Nešić, 'Key issues related to modelling of internal corrosion of oil and gas pipelines – A review', *Corrosion Science*, vol. 49, no. 12, pp. 4308-4338, 2007.
25. R. Reid et al., *The properties of gases and liquids*. New York: McGraw-Hill, 1987.
26. Imgarcade.com, 'Gallery For > Carbonic Acid Formation', 2015. [Online]. Available: <http://imgarcade.com/1/carbonic-acid-formation>. [Accessed: 13- Nov- 2015].
27. J. R. Scully, 'Polarization Resistance Method for Determination of Instantaneous Corrosion Rates', *Corrosion: The Journal of Science and Technology*, pp. 199-218, 2000.
28. C. A. S. M. D. S. C. P. S. A. Badea G.E., 'Polarisation Measurements Used for Corrosion', *Journal of Sustainable Energy*, pp. 1-2, 2010.

## APPENDICES

### Galvanic Currents

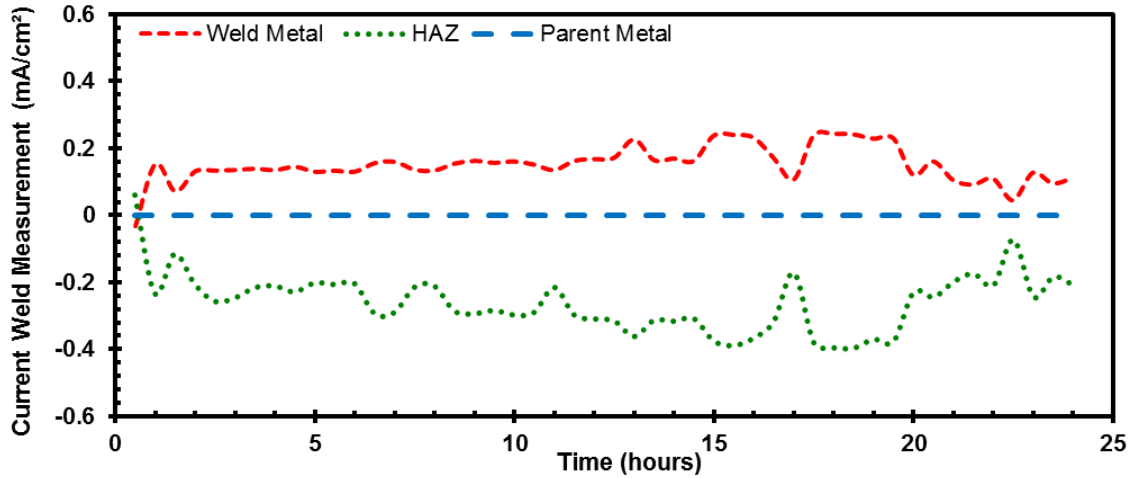


Figure 34: Test 1 current weld measurement of coupled parent, HAZ, and weld metal with time at 80°C, 3 wt. % NaCl, 0 ppm HAc and pH 4.

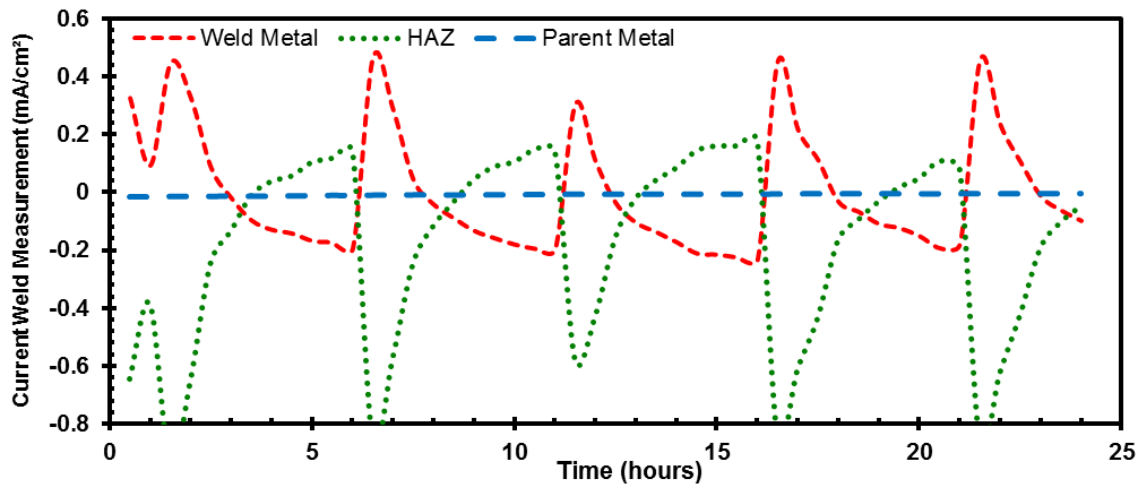


Figure 35: Test 2 current weld measurement of coupled parent, HAZ, and weld metal with time at 80°C, 3 wt. % NaCl, 0 ppm HAc and pH 6.6.

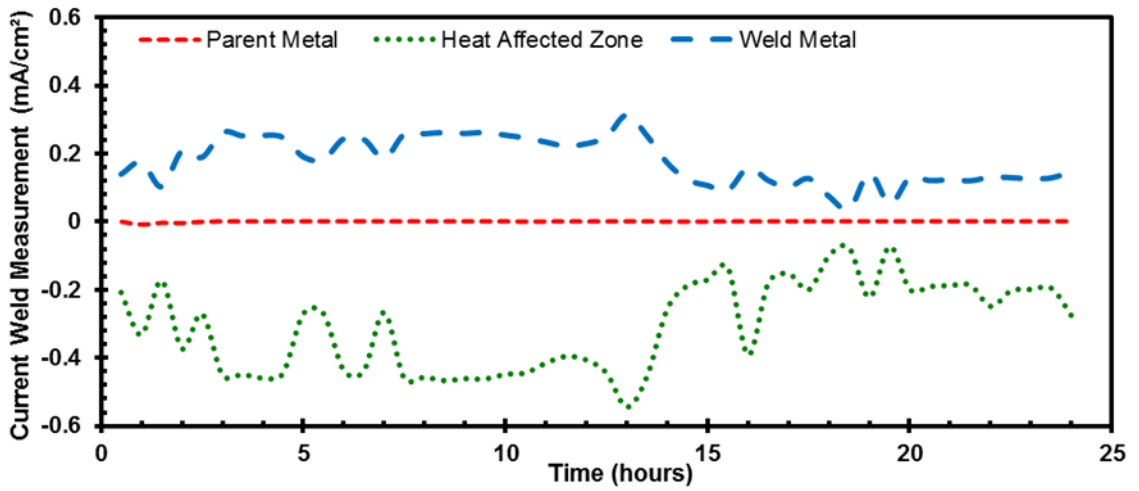


Figure 36: Test 3 current weld measurement of coupled parent, HAZ, and weld metal with time at 80°C, 3 wt. % NaCl, 1000 ppm HAc and pH 4.

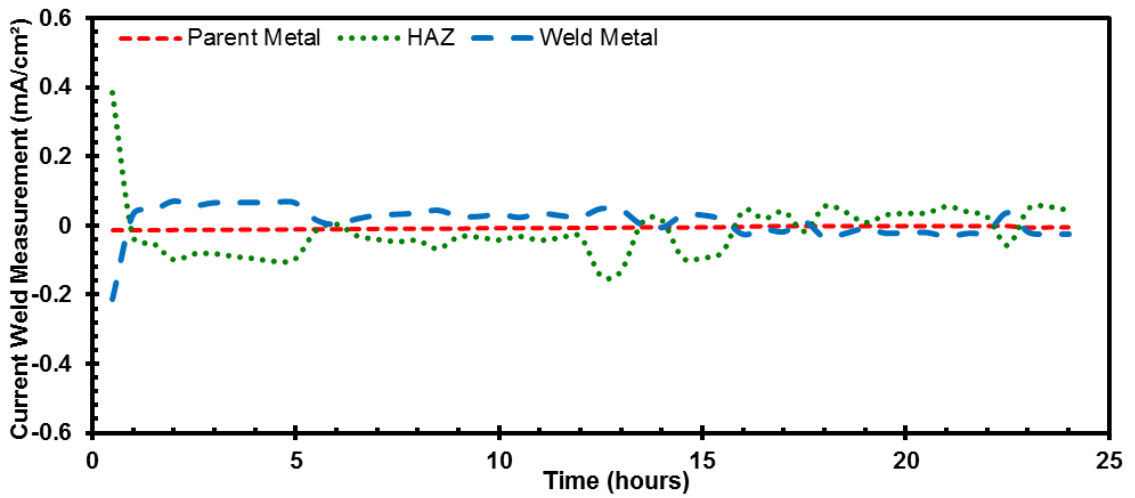


Figure 37: Test 4 current weld measurement of uncoupled parent, HAZ, and weld metal with time at 80°C, 3 wt. % NaCl, 1000 ppm HAc and pH 6.6.

Table 12: The intrinsic corrosion rate of weld segments at initial point, final point and the average.

Segment	CR <sub>cal.</sub> pre-corr [mm/yr]			CR <sub>cal.</sub> final (24 h) [mm/yr]			CR <sub>cal.</sub> average [mm/yr]		
	Parent	HAZ	Weld	Parent	HAZ	Weld	Parent	HAZ	Weld
Test 1	0.04	0.02	0.05	0.08	0.01	0.05	0.09	0.01	0.05
Test 2	0.02	0.01	0.01	0.01	0.01	0	0.01	0.01	0.01
Test 3	0.02	0	0.01	0.01	0.01	0	0.01	0.01	0.01
Test 4	0.01	0.02	0	0.03	0.02	0.02	0.01	0.02	0.01

Table 13: The galvanic corrosion rate of weld segments at initial point, final point and the average.

Segment	CR <sub>cal.</sub> pre-corr [mm/yr]			CR <sub>cal.</sub> final (24 h) [mm/yr]			CR <sub>cal.</sub> average [mm/yr]		
	Parent	HAZ	Weld	Parent	HAZ	Weld	Parent	HAZ	Weld
Test 1	0	1.27	1.12	0	2.27	1.07	0	1.98	0.96
Test 2	1.8	3.95	0.04	5.15	4.68	0.02	3.31	5.09	0.04
Test 3	0	4.71	4.84	0	5.12	5.76	0.04	5.7	4.8
Test 4	0.05	2.42	2.3	0.02	3.18	0.72	0.03	3.05	2.19